Novel approaches to mapping and ablation of supraventricular tachycardia

PhD Thesis

Dr. Róbert Pap

2nd Department of Internal Medicine and Cardiology Centre, University of Szeged

Szeged

2009

Table of Contents

Publications related to the thesis:

I. **Pap R**, Traykov VB, Makai A, Bencsik G, Forster T, Sághy L. Ablation of posteroseptal and left posterior accessory pathways guided by left atrium-coronary sinus musculature activation sequence. J Cardiovasc Electrophysiol. 2008 Jul;19(7):653-8. IF: 3.798

II. Sághy L, Makai A, Bencsik G, **Pap R**. Coexistent right- and left-sided slow pathways participating in distinct AV nodal reentrant tachycardias. Pacing Clin Electrophysiol. 2008 Oct;31(10):1348-50. IF: 1.590

III. **Pap R**, Sághy L. Convergent double potentials inside the coronary sinus during atrial tachycardia: what is the mechanism? Pacing Clin Electrophysiol. 2008 Sep;31(9):1186-8. IF: 1.590

IV. Bencsik G, **Pap R**, Sághy L. Intracardiac echocardiography for visualization of the Eustachian valve during radiofrequency ablation of typical atrial flutter. Europace. 2009 Jul;11(7):901. IF: 1.706

V. **Pap R**, Klausz G, Gallardo R, Sághy L. Intracardiac echocardiography in a case with previous failed cavotricuspid isthmus ablation. J Interv Card Electrophysiol. 2009 Apr 23. [Epub ahead of print] IF: 1.075

VI. Traykov VB, **Pap R**, Bencsik G, Makai A, Forster T, Sághy L. Ventricular location of a part of the right atrial isthmus after tricuspid valve replacement for Ebstein's anomaly: a challenge for atrial flutter ablation. J Interv Card Electrophysiol. 2009 Sep;25(3):199-201. IF: 1.075

VII. Skanes AC, Jensen SM, **Papp R**, Li J, Yee R, Krahn AD, Klein GJ. Isolation of pulmonary veins using a transvenous curvilinear cryoablation catheter: feasibility, initial experience, and analysis of recurrences. J Cardiovasc Electrophysiol. 2005 Dec;16(12):1304-8. IF: 3.285

Summary

Mapping and ablation of some specific supraventricular tachycardias remains challenging despite recent advances in catheter-based therapies. This is especially true for arrhythmia substrates in the posteroseptal space, anatomical variants and atrial fibrillation.

While some posteroseptal accessory pathways (APs) can be ablated on the tricuspid annulus or within the coronary venous system, others require a left sided approach. Electrograms recorded in the coronary sinus (CS) have a smaller, blunt component from left atrial (LA) myocardium, and a larger, sharp signal from the CS musculature. In patients undergoing ablation of a posteroseptal AP we examined CS recordings during retrograde AP conduction and found a sharp potential from the CS preceding the LA blunt component in 95% of APs ablated by a right sided approach. The reverse sequence was recorded in 95% of patients with a left endocardial AP. We concluded, that the sequence of LA-CS musculature activation can differentiate posteroseptal APs that require left heart catheterization from those that can be eliminated by a totally venous approach.

We demonstrated that the CS musculature can participate in atrial macroreentry and that this produces a peculiar electrogram pattern recorded in the CS.

We provided support for the role of the posterior nodal extensions -a posteroseptal arrhythmia substrate, which is located on both sides of the septum in most hearts- in AV nodal reentry tachycardia (AVNRT) by demonstrating that right- and left-sided slow pathways can participate in distinct right- and left-sided circuits of slow-fast AVNRT in the same patient.

We also demonstrated that phased-array intracardiac echocardiography by providing real-time visualization of the anatomy can guide CTI ablation in difficult cases because of previous surgical intervention or uncommon anatomic variants.

We tested the feasibility and efficacy of a novel, curvilinear crythermic ablation catheter for isolation of the pulmonary veins (PVs) in patients with atrial fibrillation (AF). Complete pulmonary vein isolation was achieved in 91% of PVs by cryoablation. Follow up computed tomography scans at 3 months showed no PV stenosis. Twenty-two percent of patients were without recurrence of AF, and 39% had >90% reduction in symptoms without antiarrhythmic drugs. Eight patients underwent repeat study showing 93% of previously isolated veins to have recovery of conduction. Our initial experience with the circular cryoablation catheter

demonstrated safety and feasibility, however a modest long term efficacy, presumably due to the difficulty to produce permanent isolation of the PVs. Reducing heat load due to high flow, by occlusion of the pulmonary veins using a cryoballoon may improve results.

Introduction

Supraventricular tachycardia (SVT) is a common arrhythmia in otherwise healthy individuals and also in patients with organic heart disease (1). Different electrophysiologic mechanisms can be operative during the arrhythmia. The clinical syndrome consisting of recurrent, paroxysmal palpitations caused by a regular, usually narrow QRS tachycardia, often in otherwise healthy individuals is referred to as paroxysmal supraventricular tachycardia (PSVT). Based on data from the Marshfield Epidemiologic Study Area, the incidence of PSVT was 36/100,000 person-years and the prevalence was 2.29/1000 persons (2). The age at the onset of PSVT was variable, average age was 57 years (range: infancy to 90 years old). Women were twice more likely to develop SVT than men. More than half of the cases had concomitant cardiovascular disease, the others are referred to as having "lone" PSVT. Patients with lone PSVT were younger, developed symptoms earlier and had a higher tachycardia rate (2).

The distribution of different PSVT mechanisms also shows variability between different age groups and sexes. Based on a study of 1754 patients undergoing catheter ablation of 1856 SVTs (excluding atrial fibrillation, atrial flutter, and inappropriate sinus tachycardia) between 1991 and 2003, Porter et al found atrioventricular nodal reentrant tachycardia (AVNRT) to be the predominant PSVT mechanism (56%), followed by atrioventricular reentrant tachycardia (AVRT) (27%), and focal atrial tachycardia (17%). The proportion of AVRT in both sexes decreased with age, whereas AVNRT and AT increased (3).

Recent advances in catheter-based therapies have offered a cure for many specific SVTs (4), but difficulties remain, especially in cases of septal or paraseptal arrhythmia substrates, anatomical variants and complex SVTs like atrial flutter and fibrillation.

Mapping and ablation of SVT substrates in the posteroseptal space

The posteroseptal (or inferoparaseptal) space incorporates the converging segments of the atrioventricular (AV) rings and also the coronary sinus (CS) with its proximal branches. Arrhythmia substrates in this region include accessory pathways, the posterior AV nodal extensions (thought to constitute the slow AV nodal pathway) and focal or macroreentrant

atrial tachycardias, sometimes incorporating the musculature of the CS. This space on the right atrial side is continuous with the cavotricuspid isthmus, the major target of classical flutter ablation.

Posteroseptal and left posterior accessory pathways

Accessory pathways (APs) in this region are usually more difficult to eliminate than in other areas (5). They can be associated with any of the components of this complex space and can insert in the right or left AV ring or the CS. The CS develops from the sinus venosus, together with the smooth part of the right atrium. As a continuation of right atrial myocardium the proximal CS is covered by a cuff of striated muscle, with connections to the left atrium (6). "Atrial" electrograms recorded from inside the proximal CS originate not only from left atrial myocardium, but also from activation of the CS myocardial coat. This results in "fragmented" or double potentials, with a low amplitude, blunt ("far field") left atrial component and a larger, sharp ("near field") signal from the CS musculature (7). The myocardial coat covering the proximal CS extends to the terminal portion of the middle cardiac vein and posterior coronary vein in 3% and 2% of hearts, respectively (8). These extensions - when connected with the epicardial surface of the ventricle - are thought to constitute the so-called epicardial APs in the posteroseptal and left posterior region (9). Ablation of these APs requires energy delivery inside the CS or its proximal branches in contrast to the more common APs in this region that are successfully ablated on either the mitral or the tricuspid annulus. Mapping of both sides of the septum however prolongs procedure and fluoroscopy times and carries the risks of potentially unnecessary left heart catheterization. Therefore the ability to discriminate - without instrumentation of the left heart - APs amenable to ablation from the right side (on the tricuspid ring or inside the coronary venous system) from those requiring ablation on the mitral ring, could have great impact on the safety of the procedure. We hypothesized that the sequence of left atrial and CS myocardial coat potentials recorded during retrograde AP conduction by a catheter placed inside the CS can guide mapping of these APs into right or left sided compartments of the inferior paraseptal space.

The posterior AV nodal extensions

Experimental (10) and electrophysiological (11) studies, as well as histopathological evidence after successful ablation (12) suggest that the posterior nodal extensions (PNE) represent the anatomic substrate of slow AV nodal conduction and therefore AV nodal reentrant tachycardia (AVNRT). Out of 21 randomly selected human hearts, Inoue and Becker found 13 to have both a right- and a left-sided PNE, 7 with only right PNE and one with only left PNE (13). A right or left sided circuit of slow-fast AVNRT using either the right or the left PNE has been proposed (14), but no patient with separate left and right sided slow AV nodal pathways supporting two distinct AV nodal reentrant tachycardias has been reported previously.

Macroreentrant atrial tachycardia incorporating the CS musculature

Participation of the CS musculature in atypical flutter is a rare entity nevertheless it has been reported after left atrial ablation for atrial fibrillation (15) and one case also without a previous ablation (16). We observed a unique pattern of atrial activation in this rare arrhythmia.

Intracardiac echocardiography during cavotricuspid isthmus ablation

Classical right atrial flutter is a common supraventricular tachycardia and can be terminated by the ablation of the cavotricuspid isthmus (CTI). Anatomical variation of the CTI can present an obstacle during ablation (17). We used intracardiac echocardiography (ICE) in difficult cases of CTI ablation.

Cryoablation of pulmonary veins for the treatment of atrial fibrillation

Since the seminal observations by Haissaguerre et al (18) the pulmonary veins became the main target for ablative therapy of atrial fibrillation. However pulmonary vein stenosis complicating radiofrequency ablation for atrial fibrillation emerged as a new clinical

syndrome (19). Cryothermal ablation has the potential to cause less tissue disruption and subsequent fibrosis compared to radiofrequency energy and has been shown not to cause pulmonary vein stenosis after ablation for atrial fibrillation (20). Pulmonary vein electrical isolation using focal cryothermal catheters is feasible but associated with long procedure times, therefore we used a novel, curvilinear freezing catheter in patients with atrial fibrillation.

Aims

1. To characterize the substrate and new mapping strategies of different arrhythmias involving the posteroseptal space of the heart, including: accessory pathways, the AV nodal extensions and coronary sinus musculature.
2. To describe the role of intracardiac echocardiography for the visualization of the cavotricuspid isthmus in difficult cases of common right atrial flutter ablation
3. To demonstrate the feasibility and examine the efficacy of a novel transvenous curvilinear cryoablation catheter for the ablation of atrial fibrillation

Patients and methods

Patients included in these studies were admitted to the 2nd Department of Internal Medicine and Cardiology Centre, University of Szeged or the Arrhythmia Service, University of Western Ontario, London, Ontario, Canada for catheter ablation of SVT.

Electrophysiology study

Patients were studied under sedation using midazolam ± fentanyl. Quadripolar electrode-catheters were introduced from the right femoral vein into the right atrium, His bundle region and right ventricle. A decapolar catheter, with 2-6-2 millimeter electrode spacing was introduced via the left subclavian or right internal jugular vein into the CS. The most proximal electrode pair was positioned at the ostium, in the plane of the septum as defined by the His catheter viewed in a left anterior oblique projection. The rest of the electrodes covered

approximately the proximal 40 millimeters of the CS. Bipolar electrograms were filtered between 30 and 500 Hz and recorded by a computerized electrophysiology system (EP Workmate, EP Med Systems or Cardiolab, GE Medical Systems). Determination of tachycardia mechanisms was accomplished using activation mapping with or without an electroanatomic mapping system (CARTO, Biosense Webster), as well as resetting and entrainment maneuvers. In three cases with difficult CTI ablation a 10 Fr phased array intracardiac echocardiography (ICE) catheter (Acuson AcuNav Diagnostic Ultrasound Catheter, Siemens Medical Systems) was introduced from the left femoral vein into the right atrium to visualize the CTI.

In patients with PSVT atrial and ventricular extrastimulation was carried out to study AV conduction and induce the arrhythmia. In cases with posteroseptal or left posterior accessory pathway (AP), orthodromic AV reentry tachycardia (AVRT) was diagnosed when ventricular extrasimuli delivered during His refractoriness reproducibly terminated the tachycardia or pre-excited the atrium with unchanged atrial activation sequence (Figure 1.). In patients without inducible orthodromic AVRT the para-Hisian pacing maneuver was used to demonstrate retrograde atrial activation through the AP (21). Exclusive retrograde AP conduction beyond AV node ERP was further confirmed after ablation of the AP in these patients, by the lack of retrograde conduction at the same coupling intervals. To test the hypothesis, that the sequence of left atrial and CS myocardial coat potentials recorded during retrograde AP conduction can guide mapping, bipolar electrograms from the CS were analyzed during retrograde atrial activation exclusively through the AP - preferably during orthodromic AVRT - at a paper speed of 300 mm/s. In case of fusion of ventricular and atrial electrograms, tracings during premature ventricular stimulation (Figure 1.) or VA block were examined for comparison. Electrograms of 22 retrospectively studied patients were analyzed by an electrophysiologist blinded to the results of ablation. In the prospective phase (18 patients) the analysis was done before proceeding to ablation.

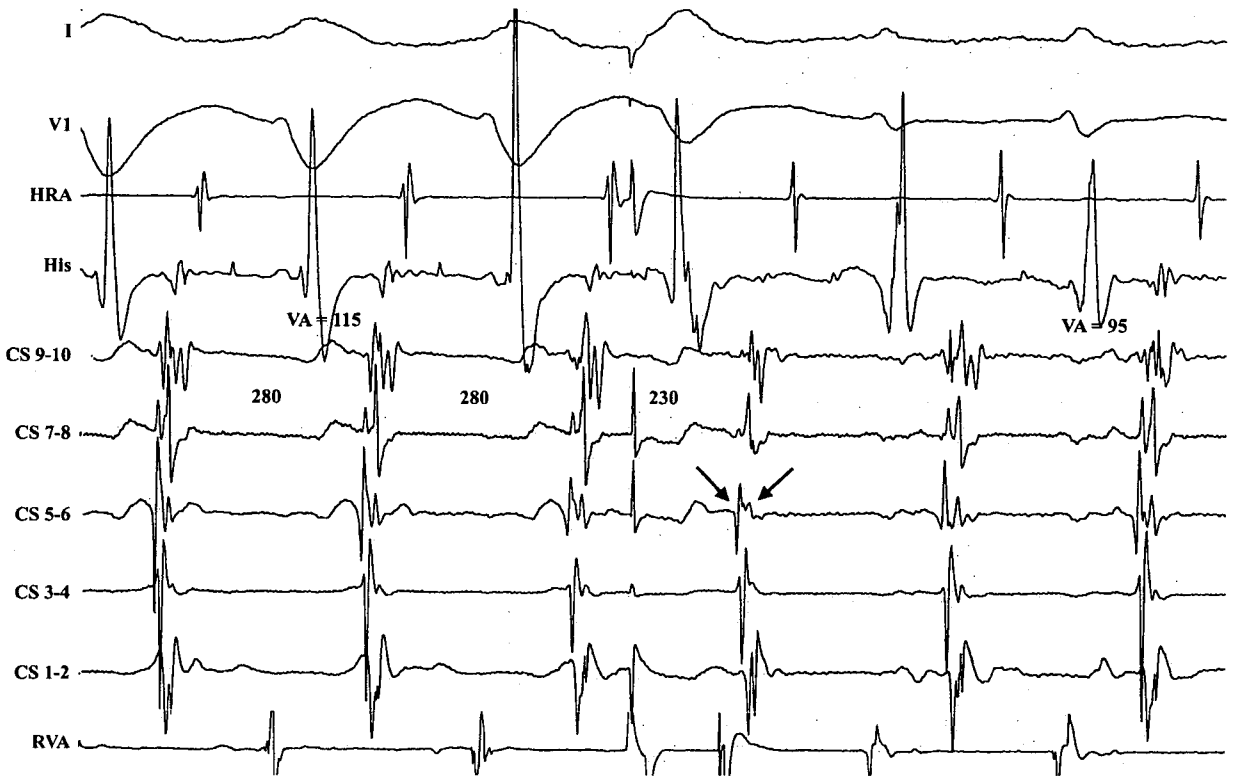

Figure 1. Surface ECG leads I and V1 with intracardiac recordings from the high right atrium (HRA), His bundle region (His), coronary sinus (CS) proximal (CS 9-10) to distal (CS 1-2) and right ventricle (RVA) are shown. Orthodromic AVRT in a patient with a CS-associated (epicardial) AP. A ventricular extrastimulus delivered during His refractoriness terminates functional left bundle branch block (LBBB) and advances the next atrial activation with unchanged sequence. Earliest "atrial" electrogram is recorded on CS 5-6, with the sharp potential from the CS preceding the smaller LA potential (arrows). The ventriculo-atrial (VA) interval is prolonged during LBBB. Paper speed is 150 mm/sec.

In patients undergoing cryoablation of pulmonary veins (PVs) double transseptal puncture was performed and systemic anticoagulation was initiated with intravenous heparin to maintain an activated clotting time between 250 and 300 milliseconds. A decapolar circular mapping catheter (Lasso, Biosense Webster) was advanced to map the PVs during sinus rhythm or distal CS pacing. The circular cryoablation catheter (Arctic Circler, CryoCath Technologies, Kirkland, PQ, Canada) was 7 F with a 64 mm freezing segment formed into a circular shape perpendicular to the shaft similar to a Lasso catheter. The freezing segment was self-expanding reaching a diameter of 18–30 mm. The catheter was positioned proximal to the Lasso catheter for monitoring the effect of cryoablation (Figure 2.). Cryoablation was

terminated if no effect was observed within 60 seconds of freezing. If a change in PV potentials occurred, lesions were continued for 4 minutes. Isolation was completed when necessary by a focal 7 F 4 mm cryoablation catheter (Freezor, CryoCath Technologies). The right lower PV was not targeted due to its small size, minimal or no electrical activity and because it was technically difficult to reach with the Lasso and the cryoablation catheter.

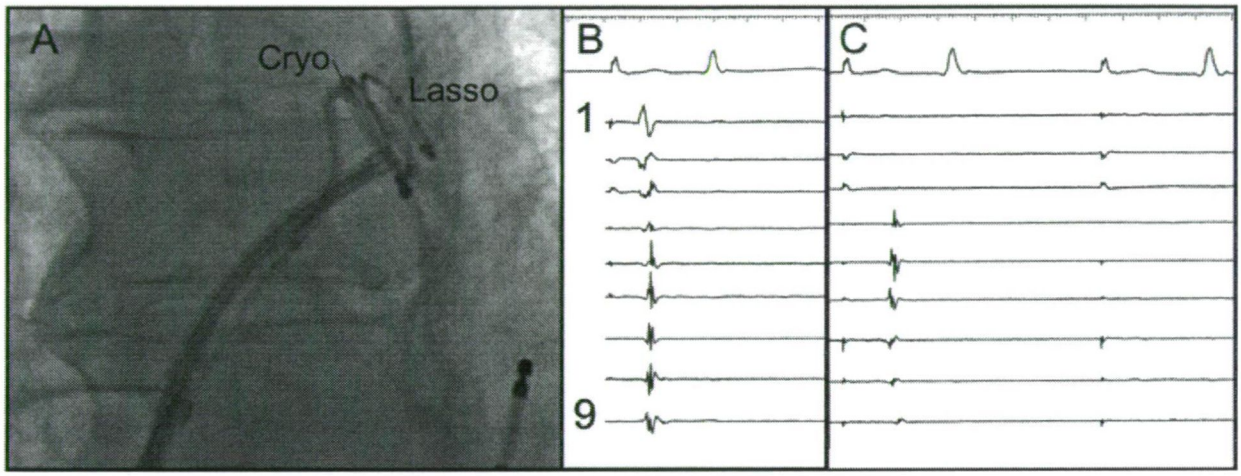

Figure 2. Pulmonary vein isolation. Panel A shows the circular cryoablation catheter (Cryo) in the left upper pulmonary vein with the circular mapping catheter (Lasso) placed distally in the vein to record pulmonary vein potentials. Panel B shows surface lead II and pulmonary vein potentials (1–9) as recorded by the circular recording catheter. Panel C shows two consecutive paced beats with sudden disappearance of the potentials approximately 30 seconds into cryothermal application.

Patients after cryoablation were monitored for 24 hours and were discharged the next day on subcutaneous low-molecular-weight heparin (LMWH) as a bridge to warfarin therapy. Patients underwent spiral CT scanning prior to ablation to delineate the anatomy and measure ostial diameter of the pulmonary veins. The CT scan was repeated three months after the procedure. Patients were scheduled for clinical follow-up at one, three and six months. All patients were followed by telephone interview every five to six months thereafter. Warfarin was discontinued after three months in patients without thromboembolic risk factors if no recurrence of AF was reported and the spiral CT scan excluded significant pulmonary vein stenosis. Antiarrhythmic drugs were discontinued in patients without recurrent AF beyond three months. AF in the first eight weeks after ablation was not considered an indicator of

therapeutic failure. Freedom from AF was defined as the absence of symptomatic AF beyond eight weeks post ablation, without antiarrhythmic drug therapy. Marked improvement in AF was considered as >90% reduction in the frequency of symptomatic episodes off all antiarrhythmic medications.

Statistical analysis. Continuous variables are expressed as mean ± SD and were compared by Student's *t*-test. A Chi-square test or Fisher's exact test was used to compare categorical variables. A p value < 0.05 was considered statistically significant.

Results

Posteroseptal and left posterior accessory pathways

Forty patients with a posteroseptal or left posterior accessory pathway (AP) were included in this study (22 analyzed retrospectively, 18 prospectively). Patient characteristics are summarized in Table 1.

Clinical characteristics
(n=40)

Age (years)	7-75 (mean 45)
Male/female	22/18
Prior ablation	10 (25%)
Pre-excitation	21 (52.5%)

Table 1.

Of the 40 APs eleven (27.5%) were successfully ablated on the tricuspid annulus and these are termed right endocardial APs. Nine (22.5%) were ablated inside the coronary venous system (epicardial APs), at the ostium of the posterior coronary vein (two patients) or the middle cardiac vein (7 patients). Twenty APs (50%) were ablated on the mitral annulus via

transseptal puncture (left endocardial APs). Ventricular pre-excitation was present during the study in 46%, 78% and 45% of the patients with a right endocardial, epicardial or left endocardial AP, respectively. Orthodromic AVRT was inducible in 37 (93%) patients. The three noninducible patients were all from the retrospective cohort. Two of them (one concealed and one manifest AP) were ablated from the left atrium, and one was ablated on the tricuspid annulus (a manifest AP).

During exclusive retrograde AP conduction, the site of earliest atrial activation recorded by the five electrode pairs of the CS catheter tended to be more leftward from right endocardial through epicardial to left endocardial APs (Figure 3.). However there was considerable overlap between groups in the mid CS.

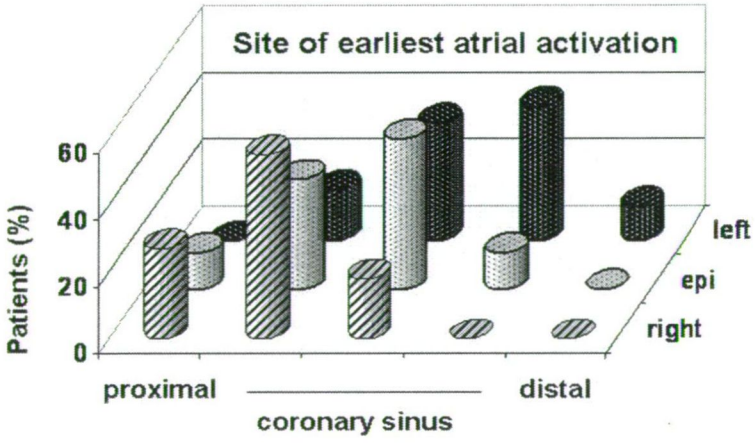

Figure 3. Distribution of the site of earliest atrial activation during retrograde AP conduction (as recorded by the five electrode pairs of the coronary sinus catheter) in patients with right endocardial (right), epicardial (epi) and left endocardial (left) APs.

The electrograms recorded at the earliest site in the CS were "fragmented" or double potentials, displaying a sharp, "near field" and a blunt "far field" component in all patients (Figures 1. and 4.). The sharp component preceded the blunt signal (sharp/blunt sequence) in all patients with an epicardial AP and in ten of eleven (91%) patients with a right endocardial AP. The reverse sequence (blunt/sharp) was recorded at the earliest site in 19 of 20 (95%) patients with a left endocardial AP. Therefore 95% of all APs accessible without left heart

catheterization were associated with a sharp/blunt sequence and 95% of APs requiring left heart access for ablation were associated with the reverse sequence.

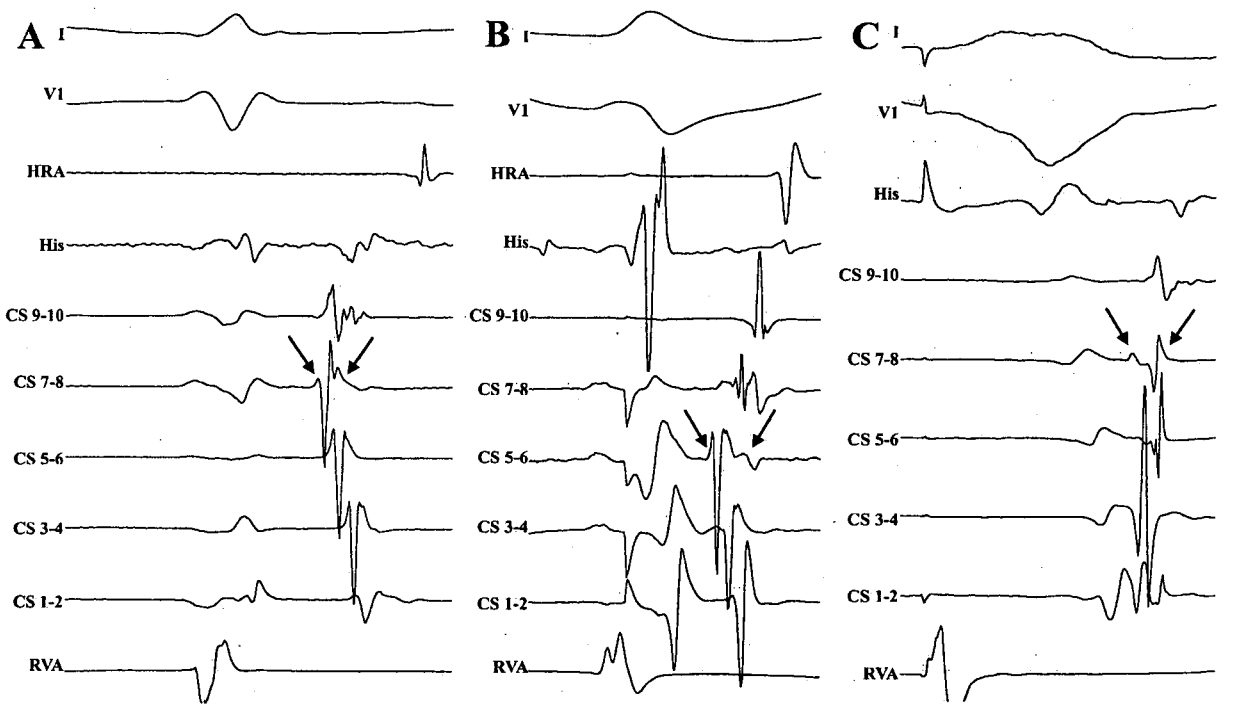

Figure 4. Representative tracings during retrograde AP conduction (leads are arranged as in Figure 1.). "Fragmented" electrogram in CS 7-8 with a high amplitude, sharp potential followed by a small, blunt component (arrows) in a patient with a right endocardial AP (A). "Atrial" double potential in CS 5-6 with sharp/blunt sequence (arrows) in a patient with epicardial AP (B). Double potential in CS 7-8 with a blunt/sharp sequence (arrows) produced by a left endocardial AP (C). Paper speed is 300 mm/sec.

Two patients were misclassified according to this scheme. The false classification of both cases presumably resulted from two relatively sharp components being recorded at the earliest site (Figure 5.).

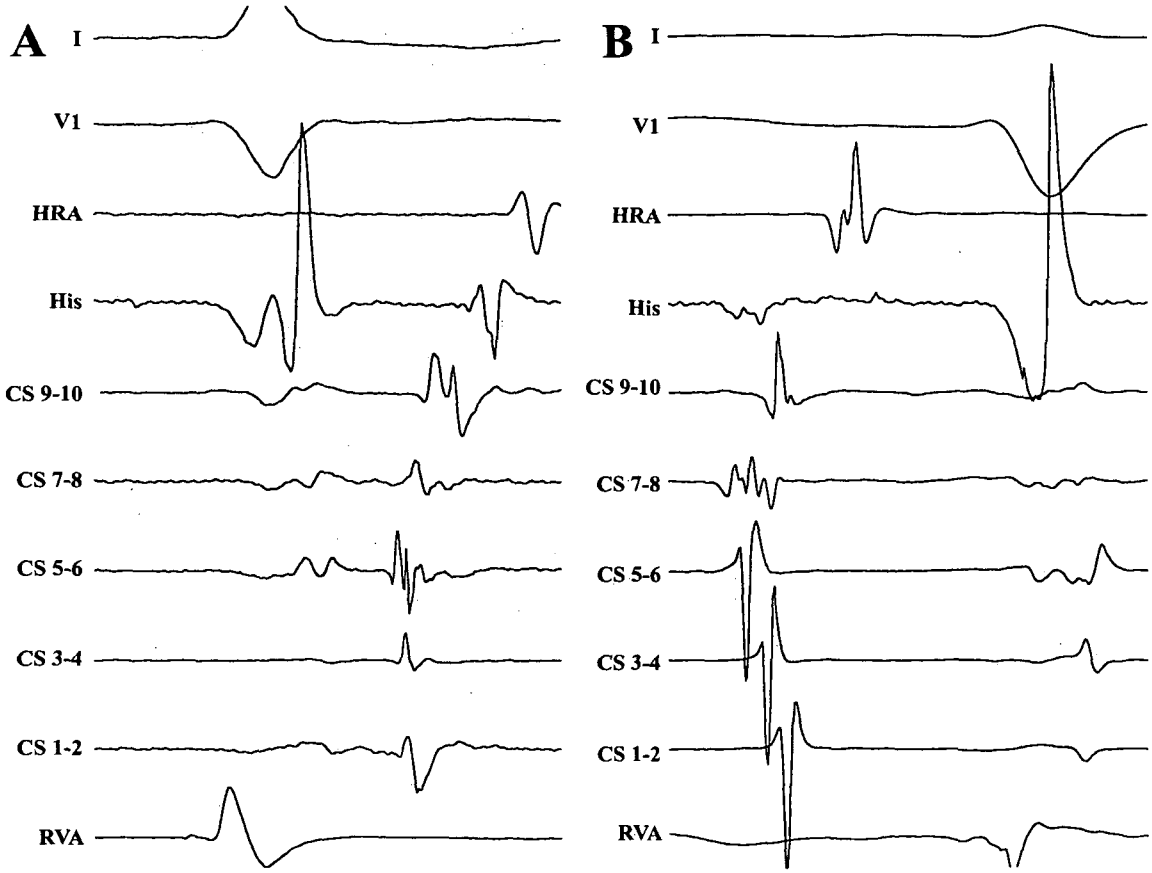

Figure 5. Tracings from the two misclassified patients (leads are arranged as in Figure 1.). "Fragmented" potential in CS 5-6, classified as sharp/blunt in a patient with a left endocardial AP (A). Complex "atrial" electrogram in CS 7-8 during long-RP AVRT, classified as blunt/sharp in a patient with a right endocardial AP (B). Paper speed is 300 mm/sec.

The posterior AV nodal extensions

A 40-year-old man with PSVT underwent an electrophysiology study. During ventricular stimulation a narrow QRS tachycardia was induced (Figure 6.) with a cycle length of 450 ms, a VA interval of -20 ms and a His to atrial (HA) interval of 40 ms. The diagnosis of AV nodal reentrant tachycardia (AVNRT) was made based on a short septal VA time and an "A-H" sequence of electrograms following termination of ventricular entrainment, excluding AV reentrant and atrial tachycardia, respectively. Earliest retrograde atrial activation was recorded at the apex of the triangle of Koch, by the His bundle catheter, suggesting the slow-fast form of AVNRT.

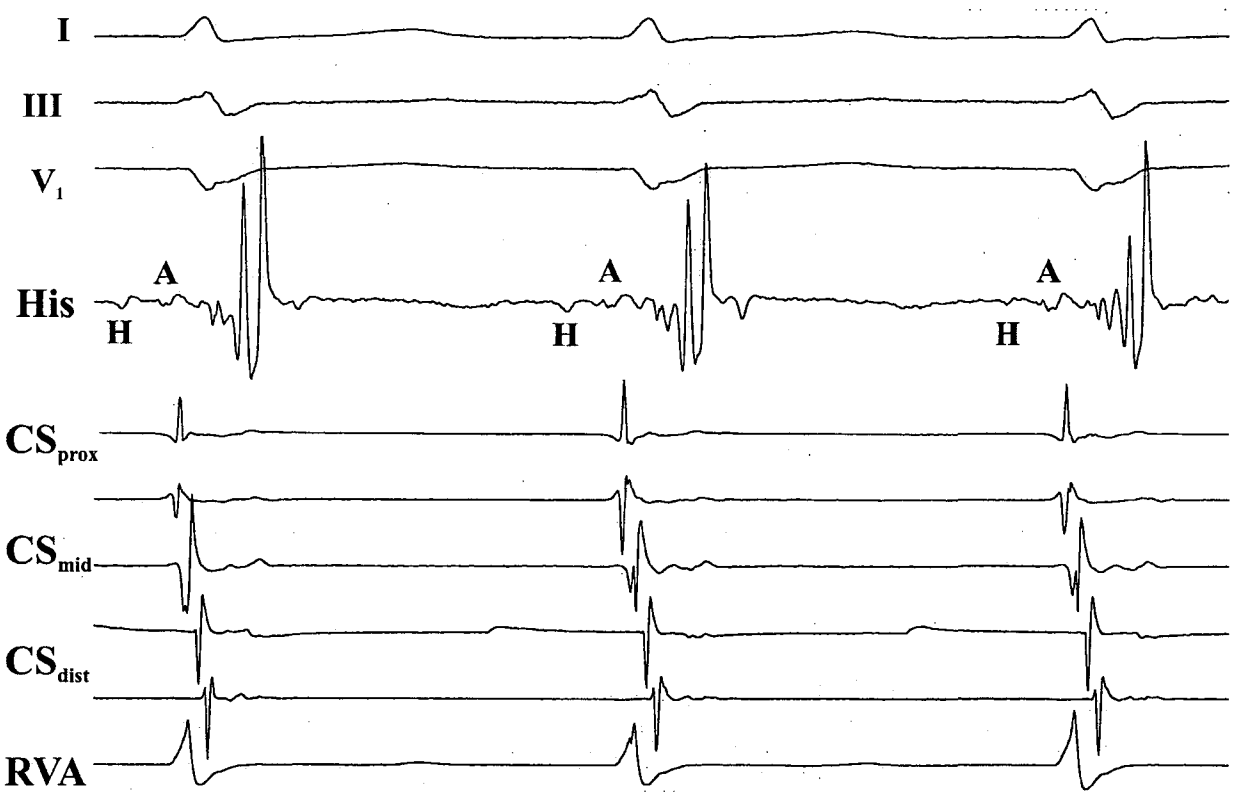

Figure 6. Surface ECG leads I, III and V_1, together with intracardiac recordings from the His bundle region (His), coronary sinus (CS) and right ventricular apex (RVA) are shown during the first tachycardia (paper speed 200 mm/s).

During atrial stimulation two discrete jumps in atrial to His (AH) interval were noted (Figure 7), with occasional induction of another tachycardia after the first jump (Figure 8).

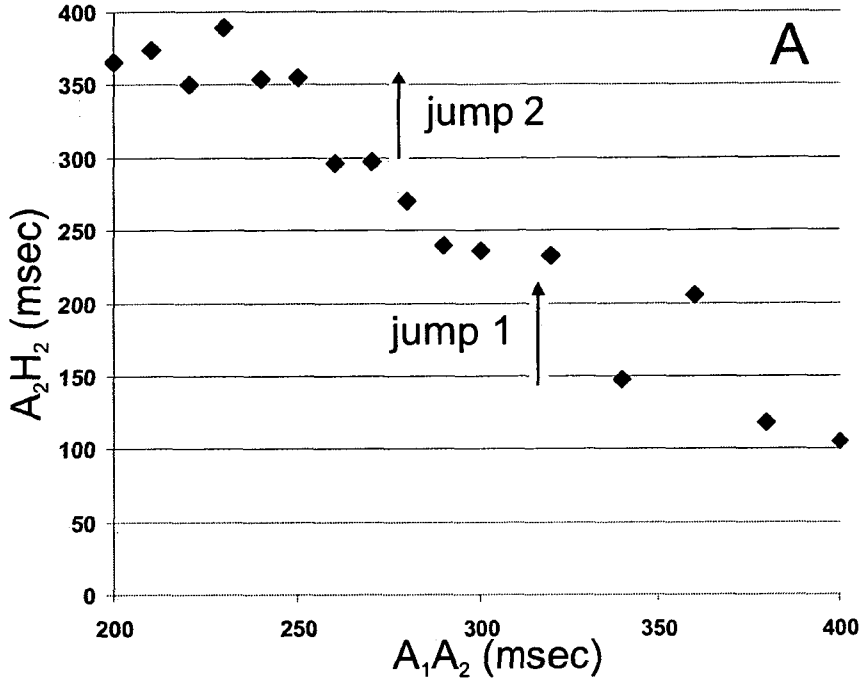

Figure 7. AV node function curve relating AH interval to atrial extrastimulus prematurity (A_1A_2) at baseline

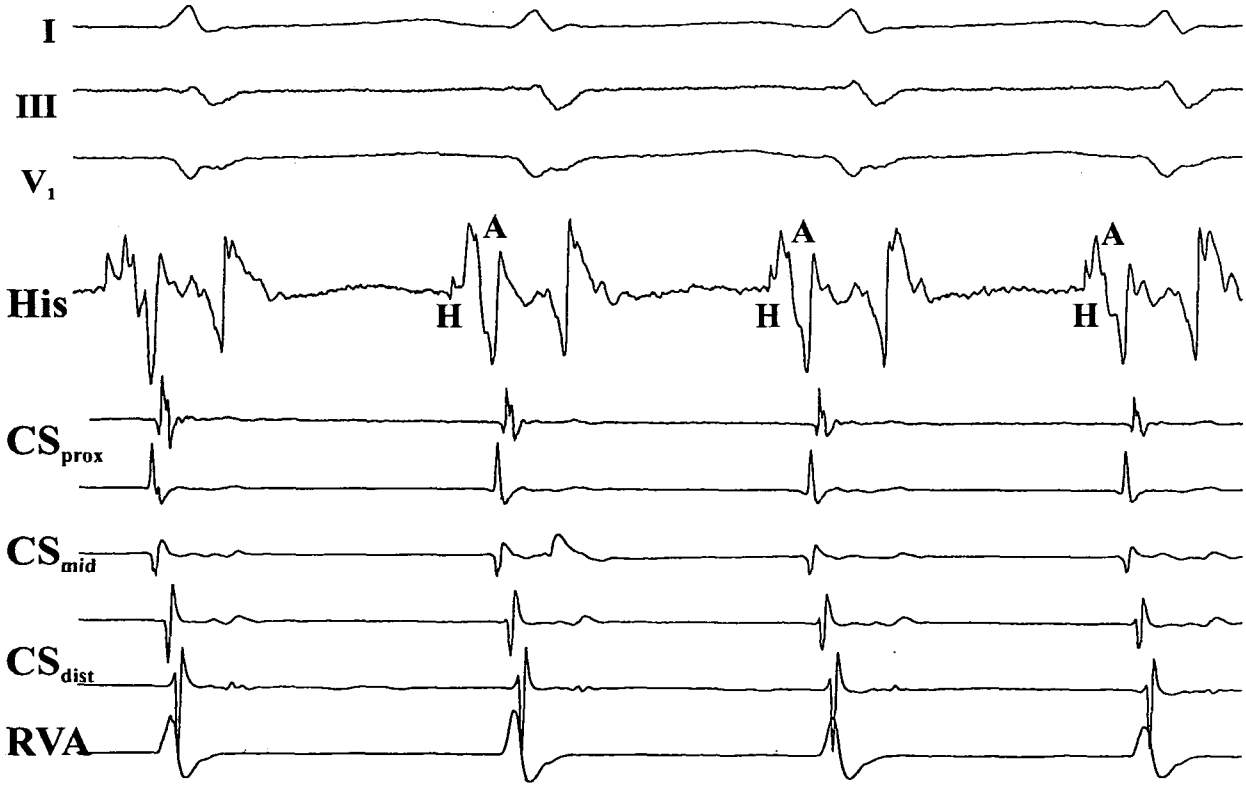

Figure 8. Intracardiac recordings during the second tachycardia (leads are arranged as on Figure 6.)

This second tachycardia proved to be also slow-fast AVNRT, with a cycle length of 320 ms, VA of -46 ms, HA of 10 ms and earliest atrial activation recorded in the His region. Radiofrequency (RF) energy delivery was carried out at the right posterior septum, with the appearance of junctional beats. During re-testing the first tachycardia was found to be non-inducible, however the second one remained easily inducible after a single jump (Figure 9.).

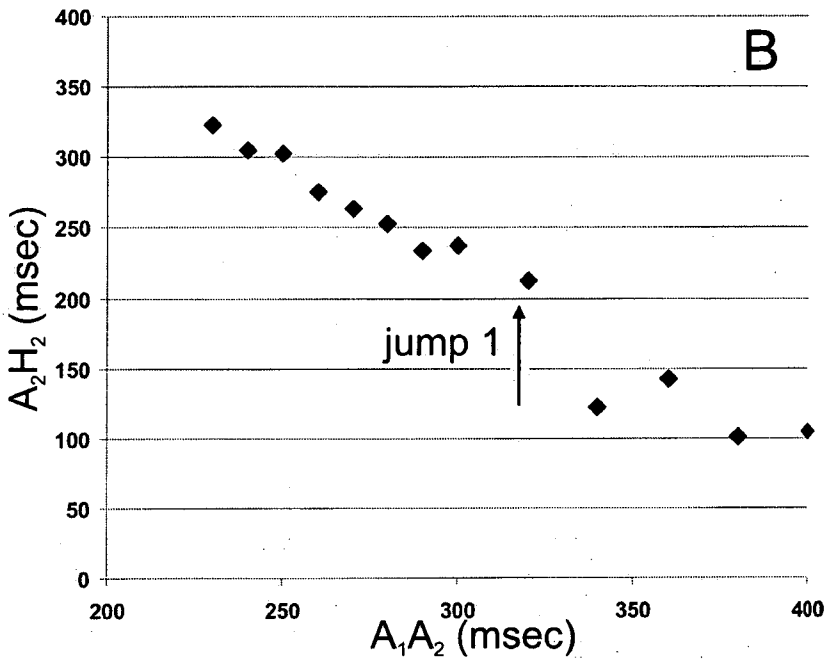

Figure 9. AV node function curve after right sided ablation

Repeated RF ablations from posterior- to mid-septum did not affect inducibility. Ablation inside the coronary sinus did not generate junctional beats. After transseptal puncture, ablation at the posteroseptal mitral annulus resulted in junctional acceleration (Figure 10.) and subsequent disappearance of slow pathway conduction (Figure 11.) and non-inducibility of AVNRT.

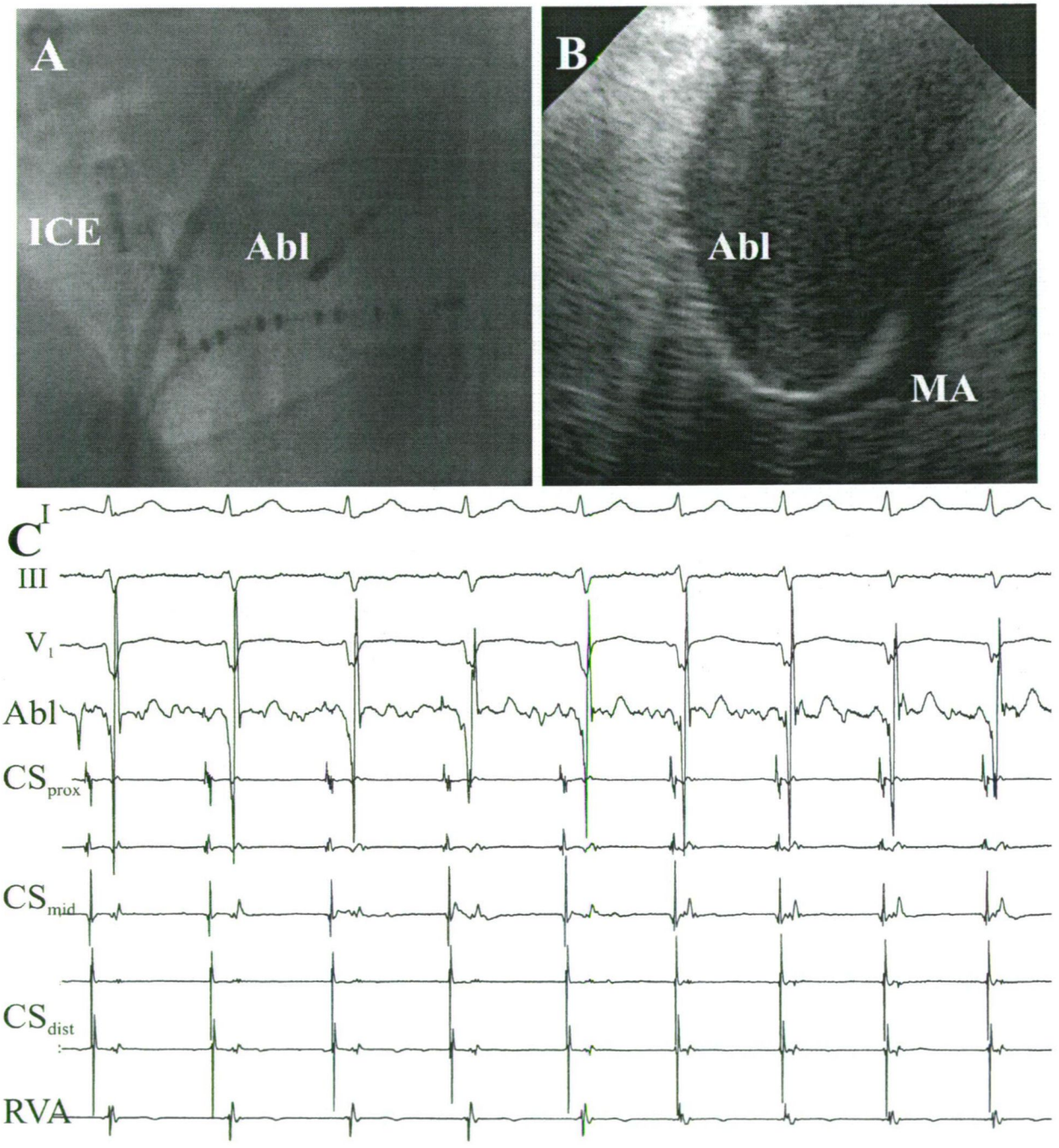

Figure 10. Fluoroscopic (A) and intracardiac echocardiographic (ICE) image (B) of the ablation catheter at the mitral annulus. Surface and intracardiac ECG tracing during RF ablation at the mitral annulus, demonstrating the generation of junctional beats (C). Leads are arranged as on Figure 6. (paper speed 50 mm/s).

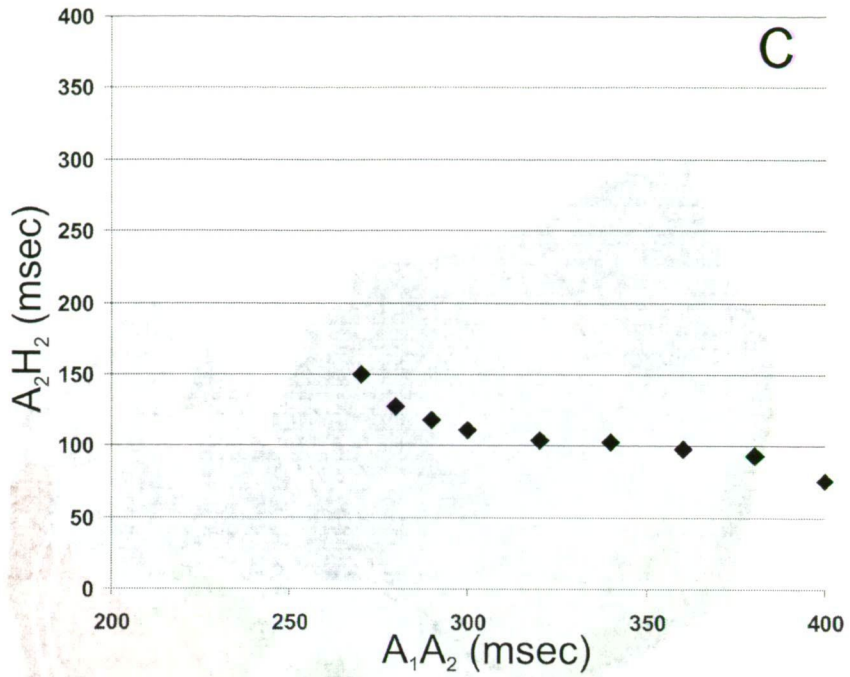

Figure 11. AV node function curve after left sided ablation

The patient remains free of palpitations ten months after the procedure. This case demonstrates that distinct right- and left-sided slow pathways, participating in right- and left-sided circuits of slow-fast AVNRT can coexist in the same patient.

Macroreentrant atrial tachycardia incorporating the CS musculature

A 61-year old man, with ischemic cardiomyopathy underwent an electrophysiology study for wide QRS tachycardia. During atrial stimulation an atrial tachycardia with a cycle length (CL) of 430 ms was reproducibly induced with a QRS morphology that was the same as during sinus rhythm and clinical tachycardia. An electroanatomic (CARTO) activation map was created of both atria during the tachycardia (Figure 12.). Entrainment pacing from the anteroseptal and posterior right atrium (RA) resulted in a post-pacing interval (PPI), equal to the tachycardia cycle length (TCL), while at the lateral RA wall the PPI was longer.

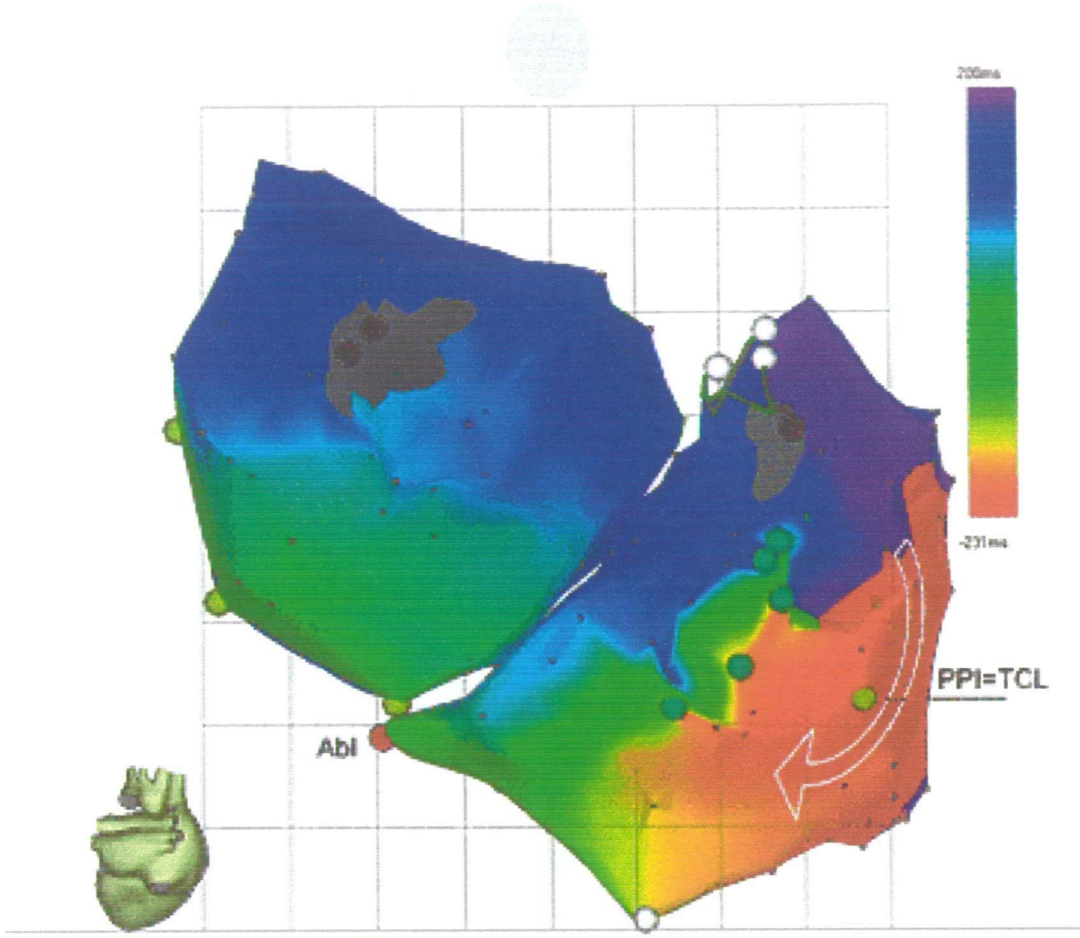

Figure 12. Posteroanterior view of the electroanatomic (CARTO) activation map of the right and left atria during tachycardia. White dots represent the caval veins. Activation proceeds around a line of double potentials (blue dots) at the posterior right atrium as indicated by the open arrow. Yellow dots indicate pacing sites. A pacing site at the posterior right atrium is marked where the postpacing interval equaled the tachycardia cycle length (PPI = TCL). At all other indicated pacing sites (along the floor of the left atrium) the PPI was longer than the TCL. A red dot marks the site of ablation (Abl) in the coronary sinus.

During entrainment from inside the proximal and mid coronary sinus (CS) endocardial activation was unchanged and the PPI was again equal to the TCL. A peculiar pattern of activation was recorded inside the CS: double potentials in the proximal portion with the two components converging up to a point in the mid CS (Figure 13A.). A premature stimulus delivered from the posteroseptal left atrium reset the tachycardia (Figure 13B.). The PPI after the extrastimulus was longer than the TCL and further lengthened with increasing prematurity of the extrastimulus.

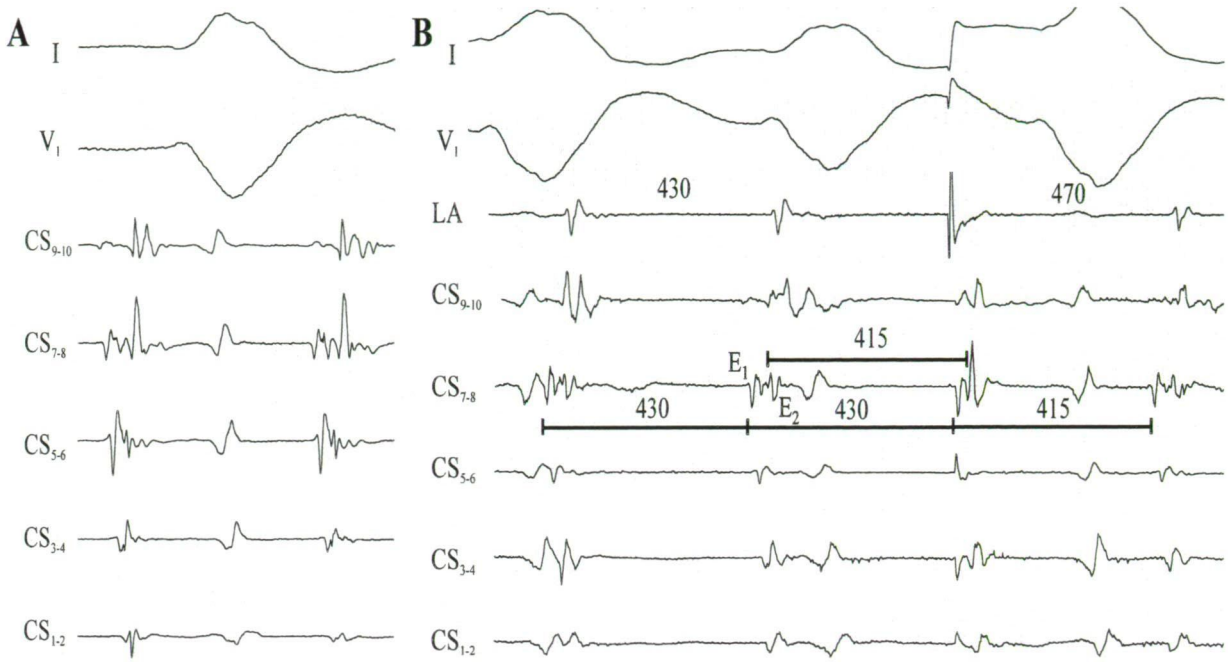

Figure 13. Surface ECG leads I and V1, together with intracardiac recordings from the proximal (CS9–10) to distal (CS1–2) coronary sinus during tachycardia (A). A premature stimulus delivered from the posteroseptal left atrium (LA) resets the tachycardia (B). The second electrogram (E2) of the double potential recorded in CS7–8 is antidromically reset (short stimulus to electrogram interval, slightly different electrogram morphology) by the extrastimulus from the LA, while resetting of the first component (E1) is orthodromic (long stimulus to electrogram interval, unchanged morphology). Postpacing interval is 470 ms. Paper speed is 150 mm/s.

Entrainment pacing yielding PPIs equal to the TCL from remote sites in the RA and CS, and a resetting response with increasing pattern point toward atrial macroreentry as the underlying mechanism of the tachycardia. Based on entrainment a portion of the right atrium was part of the reentry circuit. With CARTO activation mapping the whole flutter cycle length was represented in the RA (Figure 12.) as would be expected in case of a right atrial flutter. Nevertheless concealed entrainment was demonstrated from the proximal and mid CS with PPIs equal to the tachycardia CL, suggesting that the CS forms a protected isthmus of the reentry circuit. Recordings from inside the CS during flutter show double potentials that progressively fuse in the mid CS (Figure 13A.). A premature atrial extrastimulus delivered from the posteroseptal LA antidromically resets the second component of the double potentials while orthodromically resetting the first one (Figure 13B.). Different resetting patterns suggest that the two components of the CS double potentials are generated on either

side of the slow conduction zone of the circuit - the second component proximal and the first distal to it – and are not merely the result of local slow conduction. Being actively participating in the circuit and electrophysiologically remote from each other, we concluded that the two components represent activation of the inward and outward arms of a loop of the reentry circuit formed in the proximal CS (Figure 14.).

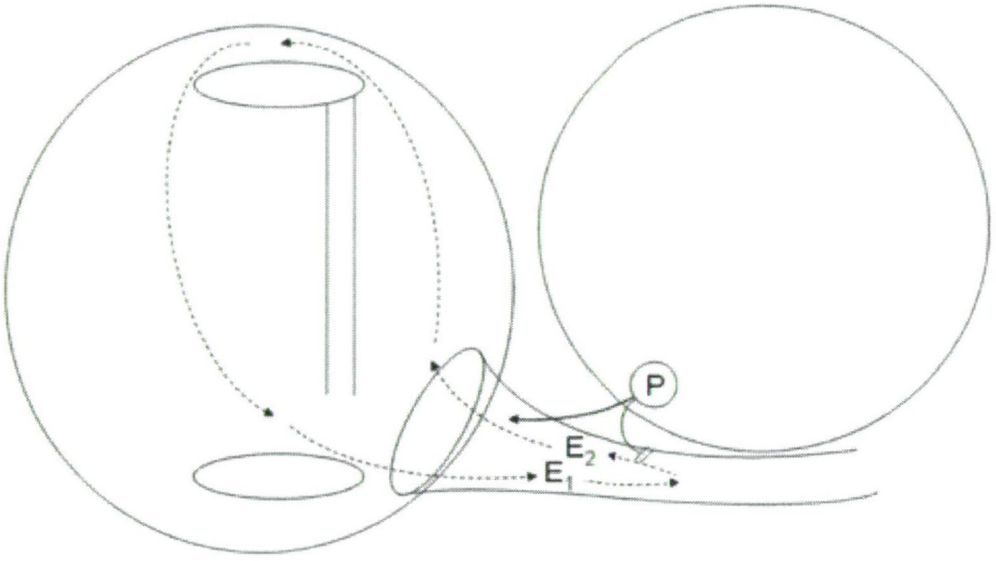

Figure 14. Schematic representation of the left and right atria and coronary sinus as viewed from a left anterior oblique projection. Long parallel lines extending from the superior vena cava represent the posterior line of block shown on the CARTO map as a line of double potentials (see Fig. 12.). The proposed reentry circuit is illustrated by the broken arrows. Double electrograms (E1 and E2) are recorded in the proximal coronary sinus during tachycardia. The solid arrows represent activation during resetting of the tachycardia by a premature stimulus delivered from a pacing site (P) in the posteroseptal left atrium (see also Fig. 13B).

The point of fusion of the two components in the mid CS was chosen as ablation target (Figure 12.). The flutter was terminated and rendered noninducible by a single application of radiofrequency current. The patient has been without recurrence for 16 months. This case represents CS musculature (with or without adjacent LA myocardium) forming a critical isthmus of atrial macroreentry otherwise confined to the RA.

Intracardiac echocardiography during cavotricuspid isthmus ablation

Intracardiac echocardiography (ICE) adequately visualized the cavotricuspid isthmus (CTI) in cases where reliance on fluoroscopy ± electroanatomic mapping (CARTO) failed.
In one of the cases a tricuspid bioprosthesis was sutured onto the CTI during corrective surgery for severe tricuspid regurgitation accompanying Ebstein's anomaly. A multislice contrast-enhanced computed-tomographic (CT) angiography revealed that the CS ostium was situated on the ventricular side of the prosthesis ring with a dilated CS draining into the right ventricle. A part of the CTI was also found to be situated subvalvularly in the functional right ventricle (Figure 15.). The patient underwent an electrophysiology study with electroanatomic (CARTO) mapping for persistent atrial flutter. Based on CARTO activation and entrainment mapping the patient was found to have clockwise CTI-dependent atrial flutter.
Radiofrequency (RF) ablation using an externally irrigated ablation catheter at the atrial side of the CTI did not terminate flutter. Since the ventricular location of a part of the circuit was strongly suspected based on CT images, lesions were delivered across the artificial valve ring, in the functional RV to complete the ablation line. This resulted in termination of the arrhythmia and subsequent bidirectional CTI block. After a 30 min waiting period CTI block was still persistent and no arrhythmias were inducible with programmed atrial stimulation.

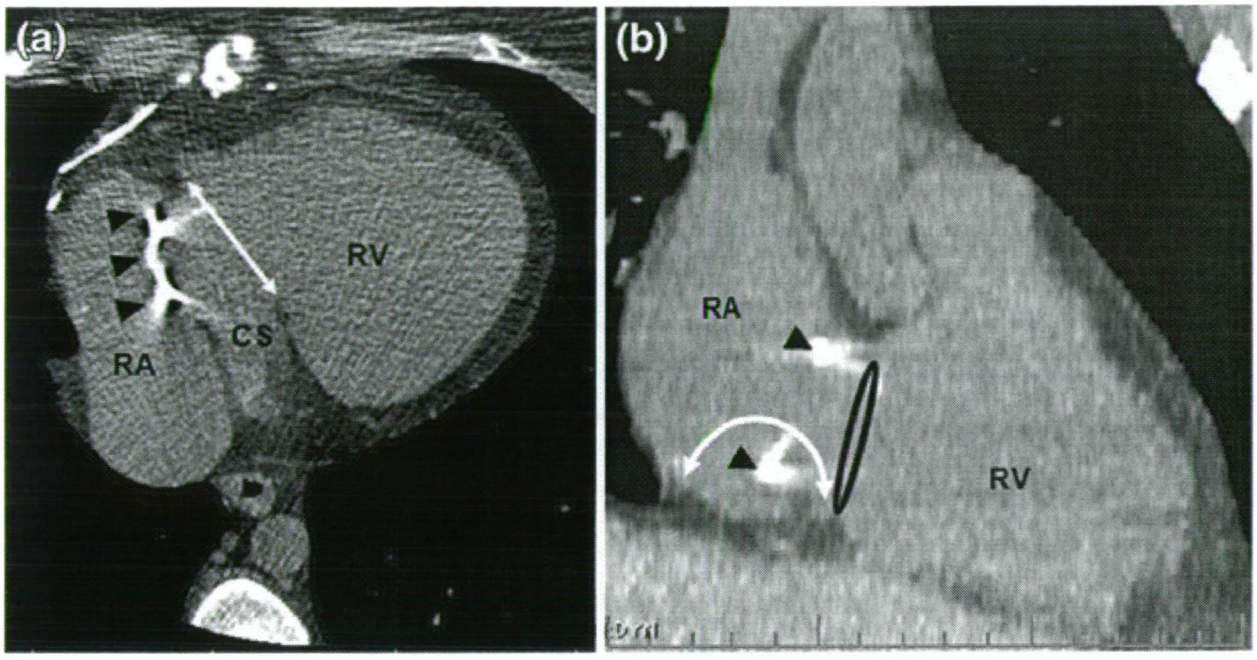

Figure15. (Panel **a**). 16 slice contrast-enhanced spiral CT image showing the CS draining into the RV under the ring of the artificial valve (arrowheads). The double arrow shows the location of the native tricuspid annulus. (Panel **b**). Reconstructed CT image corresponding to right anterior oblique fluoroscopic projection. The CTI is marked by the double arrow.

Five months after the initial procedure the patient presented with recurrent symptoms and was found to have a recurrence of AFL with the same ECG morphology. Therefore a redo procedure was performed, during which recovered conduction across the part of the CTI located in the functional RV was demonstrated. ICE imaging of the CTI (Figure 16.), the prosthetic valve ring with improved ablation catheter-tissue contact resulted in successful CTI ablation and the patient was arrhythmia free during 18 months of follow up.

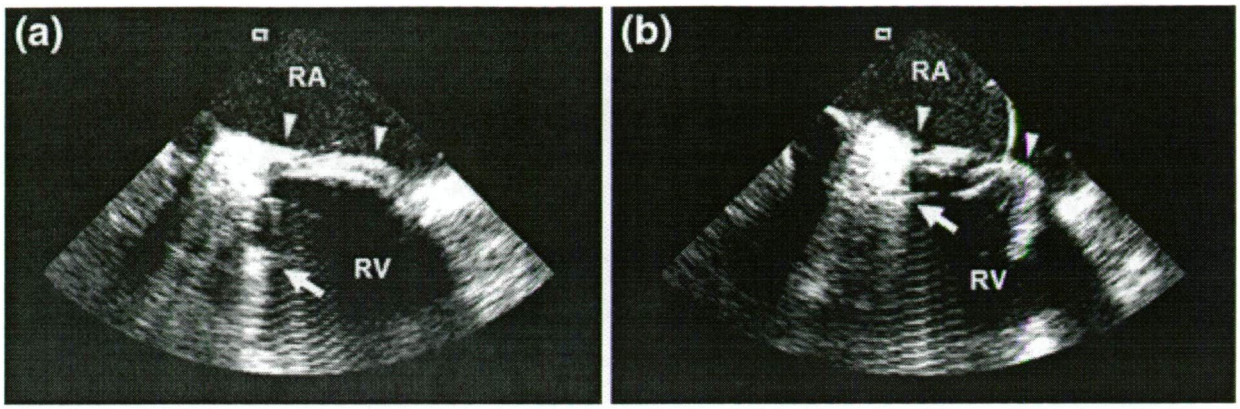

Figure 16. (Panel **a**) ICE images showing the position of the artificial valve ring (arrowheads) in the atrium. The native valve ring is marked by an arrow. (Panel **b**) The position of the ablation catheter tip (arrow) across the artificial valve on the cavotricuspid isthmus located in the functional right ventricle.

ICE imaging also proved useful in cases where an unusually prominent Eustachian ridge (ER) was the likely reason for failure of conventional CTI ablation.

In one of these cases a previous ablation session failed at another institution, where ablation of the CTI was unsuccessful despite irrigated radiofrequency (RF) ablation. ICE imaging revealed a very prominent ER, which precluded the ablation catheter from reaching the sub-Eustachian part of the CTI. The ablation catheter was curved in the right atrium and pulled down with ICE guiding to come into contact with the sub-Eustachian isthmus (Figure 17). After RF delivery at this site bidirectional CTI block was demonstrated. Conduction through the CTI recurred after a waiting period and was eliminated by further ablation at the same site.

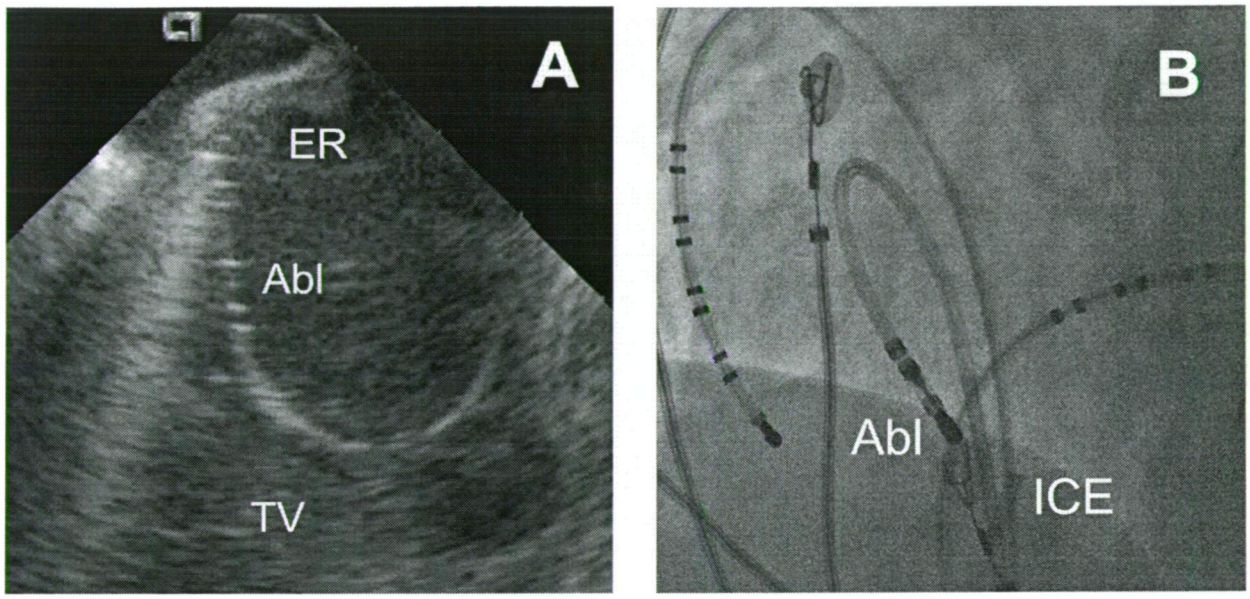

Figure 17. Intracardiac echocardiographic image (A) of the cavotricuspid isthmus. The ablation catheter (Abl) is curved around the prominent Eustachian ridge (ER). TV=tricuspid valve. Left anterior oblique fluoroscopy (B) showing the position of the ablation catheter (Abl). ICE=intracardiac echocardiography catheter.

In a similar case we found - using ICE imaging - a very prominent and actively contracting Eustachian valve as a likely cause for prolonged unsuccessful ablations at the CTI, eliminating all recordable atrial signals. Using ICE the ablation catheter was curved into full circle thus engaging the Eustachian valve and blocking CTI conduction by ablation (Figure 18).

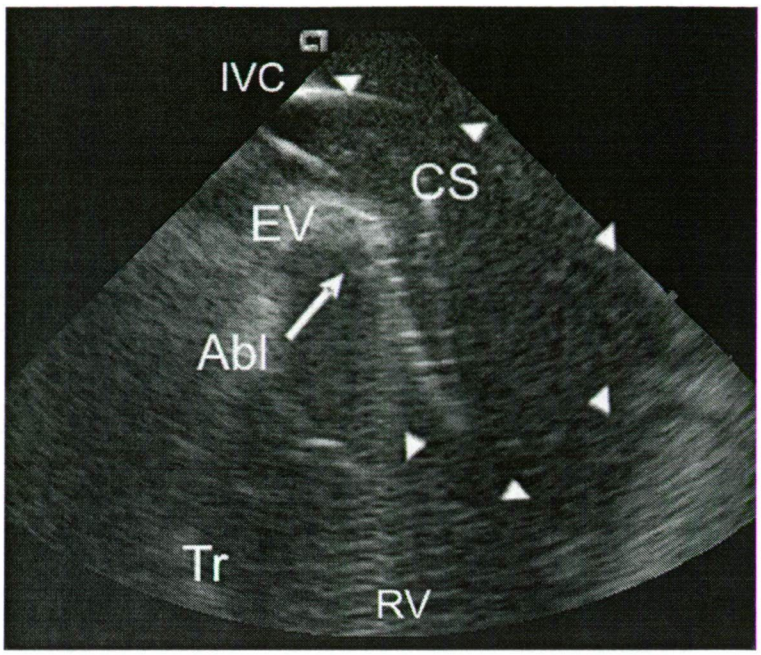

Figure 18. ICE image showing a prominent, muscular, and actively contracting Eustachian valve (EV), which could only be engaged by curving the ablation catheter (Abl) into full circle (arrowheads) to touch the anterior surface of the valve. CS, coronary sinus; Tr, tricuspid valve; IVC, inferior vena cava; RV, right ventricle.

Cryoablation of pulmonary veins for the treatment of atrial fibrillation

Eighteen consecutive patients referred for atrial fibrillation (AF) underwent cryoablation to isolate the pulmonary veins (PVs). Their clinical characteristics are summarized in Table 2.

Age (years)	52 ± 9.3
Sex (male/female)	13/5
Duration of AF (months)	69.2 ± 52.4
Frequency (episodes/month)	12.5 ± 12.1
Pattern (paroxysmal/persistent)	12/6
Number of AADs failed	3.4 ± 1.8

AF=atrial fibrillation, AAD=antiarrhythmic drug

Table 2.

PV isolation. Complete electric isolation was achieved in 18 (100%) of the 18 left upper (LUPV), 14 (88%) of the 16 right upper (RUPV), 9 (82%) of the 11 left lower (LLPV) PVs targeted (Table 3.) No ablation of the right lower PV (RLPV) was attempted by cryothermy. The mean number of cryothermic applications was 27.2 ± 11 per patient and 9.2 ± 4.7 per PV. More cryothermic energy applications (11±4.6), and longer total freezing time (26.3±9 minutes) were required to isolate the LUPV, compared to the LLPV (6.1±3 and15.4±7.7 minutes, respectively, $p<0.01$). An intermediate number of applications and freezing time (9.2±5, 20.2±9.1, $p>0.05$) isolated the RUPV. The overall mean temperature achieved during cryothermy was -79.8 ± 4 °C. There was no difference in the temperatures achieved in the three veins.

Number of PVs targeted per patient	2.5 ± 0.7
Success (isolated/targeted)	41/45 (91%)
Energy delivery time per PV (min)	21.4 ± 9.6
Procedure time per treated PV (min)	140.4 ± 48.8
Fluoro time per treated PV (min)	28.8 ± 11.9

Table 3.

In 14 (31%) of the 45 PVs targeted by cryoablation complete isolation was unsuccessful with the Arctic Circler. Incomplete isolation was equally distributed between the LUPV, RUPV and LLPV (28%, 31% and 36% of cases respectively, $p>0.05$). When analyzing failure of complete PV isolation with the Arctic Circler we found no difference between failed and successful attempts in terms of mean temperatures achieved (-78.1 vs -80.3 °C, respectively $p=0.151$), mean absolute difference in temperatures recorded by the proximal and distal thermocouple (14.1 vs 11.4 °C, $p=0.286$) or length of cryothermic energy delivery (18.05 vs 22.97 min, $p=0.112$). The cryoablation lesion created by the Arctic Circler was completed and

the vein successfully isolated by use of the Freezor focal cryoablation catheter in all ten (71%) of these PVs where it was attempted.

Complications. There were two intraprocedural complications during cryoablation of PVs. One patient developed blood pressure drop and transient ST-segment changes in inferior EKG leads during the procedure, thought to be due to air embolism into the right coronary artery and the procedure was prematurely terminated after the isolation of only the LUPV. Another patient developed right sided weakness immediately after the procedure and a left sided cerebral infarct was subsequently diagnosed by magnetic resonance imaging. Both of these patients have completely recovered after the procedure. During follow-up three patients had atrial flutter, two of them underwent successful right atrial isthmus ablation.

Follow-up. During 14.8 ± 6.2 months of follow-up four (22%) of the patients had no symptomatic recurrence of AF beyond the first 8 weeks post ablation, without any antiarrhythmic medications. One of them had documented typical atrial flutter, subsequently underwent successful right atrial isthmus ablation and has not had further symptoms. Three patients were markedly improved off all antiarrhythmic drugs after the procedure. Two of them with frequent (4 and 10 per month) persistent episodes before ablation, had one self-terminating episode of AF per year, during thirteen and 24 months of follow-up. One patient with daily paroxysmal episodes, lasting hours before the procedure, had only one or two short-lasting bouts of irregular palpitations a month, never documented to be AF, during more than a year of follow-up. Altogether 7 (39%) of the patients had their arrhythmia adequately controlled by cryoablation without the need for antiarrhythmic medications and were subsequently classified to have undergone a successful procedure. The remaining eleven patients (61%) experienced recurrence of AF despite taking one or more antiarrhythmic drugs. Nine (75%) of them stated to be clinically improved with less frequent and/or shorter episodes of AF than before the procedure. None of the patients required electrical cardioversion during the follow-up, despite 0.58 ± 0.79 previous cardioversions before ablation in this group. One patient had a permanent pacemaker implanted utilizing anti-AF algorithms. Two patients felt to be adequately controlled on medications and one progressed to asymptomatic, permanent AF. They did not wish to undergo any further invasive procedures.

Spiral CT scanning. No discrete narrowing or luminal irregularities were noted in the PVs during contrast enhanced spiral CT scanning three months after cryoablation. The mean ostial diameter of the treated RUPVs, LUPVs and LLPVs remained unchanged between baseline (14.8 ± 3.1, 14.8 ± 2.2 and 12.8 ± 1.2 millimeters, respectively) and three months (14.5 ± 2.1, 13.8 ± 2.4 and 12.7 ± 1.7 millimeters, $p>0.05$).

Repeat electrophysiology procedures. Eight (72%) of the eleven patients who failed cryoablation underwent repeat electrophysiology testing 11.3 ± 5.1 months after the first procedure. During the remapping of PVs 13 (93%) of 14 veins previously completely isolated by cryoablation had partially recovered PV potentials in 64 ± 24% of the circumference of the ostium. Four (31%) of these veins exhibited entrance block into more distal portions of the vessel. All of these PVs were successfully isolated using a large-tip RF ablation catheter.

Analysis of failures. We analyzed potential predictors of failure of cryoablation of PVs. No statistical difference could be demonstrated in baseline characteristics (Table 4.) and procedural aspects (Table 5.) between patients with and without long term success.

	Success (n=7)	Failure (n=11)	p value
Age (years)	**51 ± 11.1**	**52.6 ± 8.5**	**p=0.73**
Sex (male/female)	**6/1**	**7/4**	**p=0.6**
Duration of AF (months)	**96.4 ± 51.4**	**51.9 ± 47.3**	**p=0.08**
Frequency (episodes/month)	**12.7 ± 12.8**	**12.1 ± 12.6**	**p=0.94**
Pattern (paroxysmal/persistent)	**3/7**	**3/11**	**p=0.63**
Number of AADs failed	**1.86 ± 1.35**	**3.0 ± 1.26**	**p=0.09**
Failed amiodarone	**2 (29%)**	**7 (64%)**	**p=0.33**
LA diameter (mm)	**33.9 ± 5.3**	**34.8 ± 4.3**	**p=0.68**

Table 4.

	Success (n=7)	Failure (n=11)	p value
No. PVs targeted	2.71 ± 0.49	2.36 ± 0.81	p=0.32
No. PVs isolated	2.29 ± 0.95	2.27 ± 0.79	p=0.98
No. of cryothermic applications			
per PV	9.9 ± 2.8	12.2 ± 5.4	p=0.31
per pt	27.3 ± 10.7	27.2 ± 11.7	p= 0.99
Duration of freezing (min)			
per PV	23.1 ± 5.7	27.5 ± 11.1	p=0.35
per pt	63.5 ± 22.3	63.3 ± 27.6	p=0.99
Average temp. (°C)			
in LUPV	-79.4 ± 3.6	-81 ± 4.2	p=0.42
in RUPV	-78.3 ± 4.4	-79.8 ± 5.2	p=0.56
in LLPV	-77 ± 6.3	-83.2 ± 3.5	p=0.07
Overall average temp. achieved in targeted veins (°C)	-78.6 ± 3.7	-80.6 ± 4.2	p=0.31
Avg. prox.-dist. temp. diff. (°C)			
in LUPV	12.3 ± 8.1	9.3 ± 7.2	p=0.43
in RUPV	15.2 ± 9.7	13.5 ± 9.6	p=0.74
in LLPV	19.4 ± 11.6	8.7 ± 7.8	p=0.10
Overall avg. prox.-dist. temp. diff. in targeted veins (°C)	15.2 ± 6.9	10.8 ± 7.6	p=0.23

Table 5.

Discussion

The posteroseptal space is a complex anatomic structure where the right and left AV rings come into close proximity with each other and the proximal coronary sinus (CS). Embryologically, the CS develops from the sinus venosus, which also forms the intercaval region of the right atrium (22). As a remnant of sinus venosus musculature the proximal cca. 40 millimeter of the CS is surrounded by a cuff of striated muscle, continuous with right atrial myocardium at the CS os and having multiple connections to left atrial myocardium (6). Extensions of the CS myocardial coat to the terminal portion of the middle cardiac vein (MCV) or posterior coronary vein (PCV) can connect it to ventricular myocardium thereby forming CS-associated, epicardial APs (9). Elimination of these requires ablation of the

ventricular end at the insertion of the MCV or PCV into the CS, since ablation at the site of earliest retrograde atrial activation often produces only a change in the activation sequence due to the multiple connections of the CS myocardial coat to both atria (9). Sun et al. identified a CS-associated AP in 171 (36%) of 480 patients with posteroseptal or left posterior AP, including 39 (19%) of 201 patients without a prior ablation attempt and 132 (47%) of 273 patients with a previous failed procedure (9). The prevalence of an epicardial AP was 22.5% in our study and 30% of them had a previous ablation attempt. This highlights the difficulty of localizing these pathways.

The APs in this region are generally considered to be more difficult to eliminate than in other areas, mainly because of the difficulty of deciding whether a right or left sided approach is appropriate (5). Traditionally sequential mapping of both sides of the septum is undertaken, with ablation also carried out in the left heart or the coronary venous system if a right atrial approach fails (23). This results in long procedure and fluoroscopy times, many radiofrequency lesions and sometimes unnecessary left heart catheterization.

Coronary sinus electrograms

"Atrial" electrograms recorded by a catheter placed inside the CS originate from both left atrial myocardium and CS myocardial coat. This can lead to the recording of "fragmented" or double potentials inside the CS. Activation of left atrial musculature results in a low amplitude, blunt, "far field" potential, while CS myocardial coat activation in a higher amplitude, sharp, "near field" potential, as clearly shown in a canine model by Antz et al. (7). An activation front traveling from the posteroseptal right atrium towards the left will first activate the muscle coat covering the proximal CS, producing a large, sharp signal recorded by the electrodes inside the CS. Discrete connections of the CS musculature with the left atrium will activate left atrial myocardium, producing a lower amplitude, blunt, "far field" signal on the CS electrodes. Thus two-component "fragmented" or double potentials will be recorded in the proximal CS with the sharp component preceding the blunt signal (sharp/blunt sequence), as shown by Antz et al. by pacing posterior to the CS os (7). The same sequence is expected to happen when a retrogradely conducting AP first activates right atrial myocardium. Also the same sequence (sharp/blunt) of potentials is produced when an AP inserts directly

into the CS musculature as is the case with epicardial, CS-associated APs (9). On the other hand when Antz et al. performed pacing from the lateral left atrium the sequence was the opposite (blunt/sharp), with CS musculature activation following activation of left atrial myocardium (7). This sequence should be produced if an AP connects to left atrial myocardium, the first signal recorded in the CS being a "far field" potential followed by later activation of the CS musculature resulting in a blunt/sharp sequence of potentials (24). Different conduction velocity of left atrial myocardium and CS musculature can cause the sequence of potentials to change farther away from the insertion site of the AP explaining the importance of analyzing the electrograms recorded at the earliest site.

The recording of double potentials inside the CS has been found to be especially common during retrograde conduction through posteroseptal APs. Uchida et al. recorded fractionated or double potentials inside the CS in 11 of 12 patients with a posteroseptal AP, compared to only 13 of 39 patients with a left lateral AP (25). In our study we found "fragmented" or double potentials at the site of earliest atrial activation in the CS in all patients and showed that the sequence of these potentials can guide mapping the AP into one of three compartments of the posteroseptal space.

Comparison with previous studies

Prediction of the site of successful ablation of posteroseptal APs has been attempted by the analysis of the pre-excitation pattern on the surface ECG or the electrophysiological parameters during an invasive study. Besides the obvious limitation of the surface ECG in the case of concealed APs (47.5% in our study), reports on the accuracy of surface ECG features to differentiate APs associated with the three compartments of the inferior paraseptal space have been conflicting. Localization of manifest APs into either the right or the left heart had traditionally been achieved by analysis of the delta wave or QRS polarity in lead V_1 (26, 27). Nevertheless in a study by Dhala et al. most posteroseptal APs producing positive delta wave and QRS complex in lead V_1 were ablated at the tricuspid annulus or within the proximal CS (28). Arruda et al. reported a negative delta wave in lead II to be a highly specific finding for epicardial APs in this region (9), but later the same group found this to be the case in only 68% of CS-associated APs (29). Others have shown a negative delta wave in lead II to be

relatively common with left endocardial APs also (30, 31). A positive delta wave in lead aVR was found in these studies to be highly specific for CS-associated APs, but sensitivity was low. The differentiation between epicardial and left endocardial APs was felt to be most difficult by the authors (31).

Invasive electrophysiologic findings can also be misleading. The prolongation of the VA interval in response to the development of left bundle-branch block during orthodromic AVRT has been regarded as suggestive of a left-sided AP. However many posteroseptal APs associated with this phenomenon can be ablated from the right side (28) (Figure 1.), sometimes even when the prolongation is longer than 30 milliseconds (32).

Chiang et al. developed an algorithm for predicting the successful ablation site of concealed posteroseptal APs using multiple electrophysiologic parameters recorded during an invasive study (33). If earliest atrial activation during AVRT was in the middle CS this algorithm predicted a left endocardial ablation site. Of note is that none of the APs in this study required ablation inside the CS. This could account for the discrepancy with other studies showing that CS-associated epicardial APs can produce not only posteroseptal, but left posterior AV connections (9), rarely even with earliest retrograde atrial activation in the distal CS (34). In a study by Gatzoulis et al. more than one third of patients with an earliest site distal from the CS os required ablation inside the CS after a failed left endocardial approach (35). In our series a similar 29% of APs with earliest atrial activation at or distal to the mid CS were ablated by a venous approach, and 35% of all APs ablated from the right side produced such an eccentric retrograde atrial activation (Figure 3.). Therefore the ability of the site of earliest atrial activation during AVRT to predict the successful approach seems very limited, mainly because CS-associated APs can produce a very much eccentric retrograde atrial activation sequence.

A second criterion in the algorithm of Chiang et al. was a long-RP AVRT defining a right endocardial AP (33). This is in contrast with numerous reports of left sided, slowly conducting APs participating in the so called permanent form of junctional reciprocating tachycardia (36, 37, 38). We have seen three long-RP tachycardias in our series of patients. Two of them had earliest atrial activation recorded in the middle CS, one was ablated from the right, the other from the left atrium. Only one patient with long-RP tachycardia had earliest

atrial activity close to the CS os, the AP was ablated from the right endocardial approach in this case.

If none of the above two criteria (eccentric retrograde activation and long-RP tachycardia) were fulfilled, the algorithm by Chiang et al. required the measurement of the ΔVA interval during AVRT, which is the difference of VA intervals measured at the His catheter and the site of earliest atrial activation in the CS (33). If this interval was ≥25 ms the algorithm predicted a left endocardial AP. We retrospectively tested this third criterion of Chiang et al. on all of our patients with inducible orthodromic AVRT (without considering the first two criteria). The ΔVA interval was ≥25 ms in 89% of patients with a left endocardial AP and less than 25 ms in 95% of patients with a right endocardial or epicardial AP. This suggests that atrial activation is relatively early in the His region during retrograde conduction through both right endocardial and CS-associated APs, compared to left endocardial ones. Therefore the third criterion of Chiang et al.: measurement of the ΔVA interval during orthodromic AVRT might prove to be useful (without the first two criteria) for predicting the successful approach.

Clinical implications

The sequence of left atrium-coronary sinus musculature activation determined by a closer look at the earliest "atrial" electrograms in the CS during retrograde AP conduction can predict the successful approach for ablation of posteroseptal or left posterior APs. This might have great significance by reducing procedure and fluoroscopy times, the number of unsuccessful radiofrequency applications and preventing unnecessary mapping of the left side of the septum along with the potential complications of left heart access (39).

The posterior AV nodal extensions

Katritsis and Becker proposed a right or left sided circuit of slow-fast AVNRT using either the right or the left posterior nodal extension (PNE) (14). We demonstrated that distinct right- and left-sided slow pathways, participating in right- and left-sided circuits of slow-fast AVNRT can coexist in the same patient. The above investigators also suggested the theoretical possibility of both left and right circuits participating simultaneously in double-

loop reentry, although the left PNE is much shorter in length than the right (13), therefore - assuming similar conduction velocities - the shorter circuit on the left should have a shorter cycle length, precluding dual loop reentry. This was also confirmed by our case, where the left sided circuit of AVNRT had a shorter cycle length, than the right sided one. These observations provide further support to the role of the PNEs in slow pathway conduction.

Macroreentrant atrial tachycardia incorporating the CS musculature

Not only can the coronary sinus (CS) musculature participate in accessory pathway conduction, but - as we demonstrated - it can take part in atrial macroreentry. Participation of the CS musculature in atypical flutter has been reported after left atrial ablation for atrial fibrillation (15) and one case also without a previous ablation (16). We observed a unique pattern of atrial activation recorded by the CS catheter during the tachycardia: double potentials in the proximal CS, which fused in the mid CS. Resetting techniques demonstrated the two potentials to be generated by different arms of the reentry circuit, which involved part of the right atrium and the CS musculature itself.

Intracardiac echocardiography during cavotricuspid isthmus ablation

Anatomical variation of the cavotricuspid isthmus (CTI) can present an obstacle to catheter ablation of typical atrial flutter (17). We demonstrated that intracardiac echocardiography (ICE) in these cases can adequately visualize the CTI, the anatomical obstacle, the ablation catheter and tissue contact. The Eustachian ridge (ER) forms an elevation on the CTI dividing it into two portions: the first between the tricuspid valve and the ER (sub-Eustachian isthmus) and then from the crest of the ER to the inferior vena cava. A prominent ER can be behind the inability to reach the sub-Eustachian portion of the CTI using the usual catheter position. In this case ICE can visualize the ER and a curved catheter can reach behind the ER to ablate the sub-Eustachian isthmus. The ER can also harbor cardiac muscle fibers that can be responsible for residual CTI conduction. ICE shows active contraction of the prominent ER in this case. Difficult ablation and recurrence of CTI conduction can occur from a previous surgical procedure involving the CTI. Surgery aimed at reducing right atrial size in Ebstein's anomaly can result in the ventricular location of a part of the CTI. This is also adequately recognized during ICE imaging and ablation guided by ICE at the ventricular part can persistently block CTI conduction.

Cryoablation of pulmonary veins for the treatment of atrial fibrillation

Pulmonary vein (PV) electrical isolation has emerged as an effective treatment of paroxysmal atrial fibrillation (AF) (40). However recovery of PV conduction may occur as often as in 80% after radiofrequency (RF) ablation, contributing significantly to recurrence of AF (41). The high reconnection rate after RF ablation is related in part to the reluctance to use higher power in the region of the PVs to avoid stenosis as well as the posterior left atrium to minimize the risk of catastrophic esophageal injury (42). These potential complications have renewed interest in alternative and potentially safer energy sources for ablation of pulmonary venous and left atrial tissue. Cryothermal lesions are known to maintain the extracellular collagen matrix and produce less tissue disruption and thrombus formation (43). Similar to the results of Tse et al. (20) we did not detect any evidence of PV stenosis after cryoablation during routine CT scanning. Surgical cryothermy has been used safely for many years without

reported esophageal injury, unlike RF ablation (44). These experiences make catheter based cryothermic ablation an attractive alternative to RF, with potentially less complications.

Efficacy of cryoablation

Our initial experience with the circular cryothermal catheter demonstrates a moderate efficacy. The success rate using the cryoablation catheter was likely limited by the number of veins isolated per patient and the learning curve associated with a new catheter. Reconnection of PVs probably due to inadequate lesion depth resulting in the failure to achieve permanent PV disconnection was invariably observed after clinical recurrence. The efficacy in the current series is similar to that published using a focal cryoablation technique (20), but with shorter procedure and fluoroscopy times.

A recent worldwide survey of results using RF catheter ablation for AF has documented drug-free success rates of approximately 30–64%, depending on experience (45). Success rate in experienced centers is around 70% in case of paroxysmal AF (40). Based on these, RF appears to be more effective at producing permanent PV isolation (46). With RF, pulmonary venous flow acts to cool the catheter tip and may promote deeper lesions. In contrast, the heat load associated with ongoing PV flow limits the ability to develop deep, continuous, and permanent lesions with cryothermy. The circular catheter design allows pulmonary venous flow to continue through the centre of the cooling segment. This may further allow warming of the freezing segment. This technical consideration may also contribute to incomplete isolation. Cryothermal lesion production could be greatly enhanced by limiting heat load, using a cryothermal balloon, which results in occlusion of PV flow during freezing (47). The short term success rate using this cryoballoon was similar to that of RF ablation (48). Clinical trials are underway to determine the long term efficacy of this new technology.

New observations of the studies

1. Careful observation of coronary sinus (CS) recordings during retrograde conduction through posteroseptal or left posterior accessory pathways, with the aim to determine the sequence of activation of the CS musculature and the left atrium is useful to establish before left heart catheterization whether a right or left sided approach to AP ablation is appropriate. The CS musculature can participate in atrial macroreentry producing a peculiar pattern of double potentials recorded along the CS. The left and right posterior AV nodal extensions - both present in most hearts - can support distinct left- and right sided circuits of AV nodal reentry tachycardia in the same patient.
2. Intracardiac echocardiography is helpful when conventional ablation of the cavotricuspid isthmus fails because of a very prominent and/or actively contracting Eustachian ridge or previous surgical intervention on the tricuspid valve.
3. Pulmonary vein (PV) isolation is feasible and safe using a circular cryothermic ablation catheter for the treatment of atrial fibrillation. However long term success is limited by a high rate of reconnection of PVs, likely due to the heat load generated by ongoing PV flow during freezing.

Conclusion

Advances in mapping and technology improve the success and safety of catheter ablation for tough to get supraventricular tachycardias.

Mapping for diverse arrhythmia substrates: accessory pathways, the AV nodal extensions and macroreentry circuits in the complex posteroseptal space is facilitated by careful interpretation of electrograms and understanding of the underlying anatomy, especially the coronary sinus musculature and the biatrial nature of the AV nodal extensions.

Advanced imaging using intracardiac echocardiography allows successful ablation when a conventional approach fails because of a previous surgical intervention or uncommon anatomical variant.

Cryothermic ablation is a promising new technology for the treatment of paroxysmal atrial fibrillation, with likely less risk compared to radiofrequency, however strategies to decrease

heat load and increase lesion production are needed to achieve permanent electrical isolation of the pulmonary veins with cryothermy.

References:

1. Campbell RW. Supraventricular tachycardia. Occasional nuisance or frequent threat? Eur Heart J. 1996 Jul;17 Suppl C:21-5.
2. L.A. Orejarena, H. Vidaillet Jr and F. DeStefano et al. Paroxysmal supraventricular tachycardia in the general population. J Am Coll Cardiol **31** (1) (1998), pp. 150–157.
3. M.J. Porter, J.B. Morton and R. Denman et al., Influence of age and gender on the mechanism of supraventricular tachycardia, Heart Rhythm **1** (4) (2004), pp. 393–396.
4. 2. Lee KW, Badhwar N, Scheinman MM. Supraventricular tachycardia--part I. Curr Probl Cardiol. 2008 Sep;33(9):467-546.
5. Schluter M, Geiger M, Siebels J, Duckeck W, Kuck KH. Catheter ablation using radiofrequency current to cure symptomatic patients with tachyarrhythmias related to an accessory atrioventricular pathway. Circulation. 1991 Oct;84(4):1644-61.
6. Chauvin M, Shah DC, Haïssaguerre M, Marcellin L, Brechenmacher C. The anatomic basis of connections between the coronary sinus musculature and the left atrium in humans. Circulation. 2000 Feb 15;101(6):647-52.
7. Antz M, Otomo K, Arruda M, Scherlag BJ, Pitha J, Tondo C, Lazzara R, Jackman WM. Electrical conduction between the right atrium and the left atrium via the musculature of the coronary sinus. Circulation. 1998 Oct 27;98(17):1790-5.
8. von Ludinghausen M, Ohmachi N, Boot C. Myocardial coverage of the coronary sinus and related veins. Clin Anat. 1992; 5: 1–15.
9. Sun Y, Arruda M, Otomo K, Beckman K, Nakagawa H, Calame J, Po S, Spector P, Lustgarten D, Herring L, Lazzara R, Jackman W. Coronary sinus-ventricular accessory connections producing posteroseptal and left posterior accessory pathways: incidence and electrophysiological identification. Circulation. 2002 Sep 10;106(11):1362-7.
10. Medkour D, Becker AE, Khalife K, Billette J. Anatomic and functional characteristics of a slow posterior AV nodal pathway: role in dual-pathway physiology and reentry. Circulation. 1998 Jul 14;98(2):164-74
11. Katritsis DG, Becker AE, Ellenbogen KA, Karabinos I, Giazitzoglou E, Korovesis S, Camm AJ. The right and left inferior extensions of the atrioventricular node may

represent the anatomic substrate of the slow pathway in the human. Heart Rhythm 2004;1:582–586.

12. Inoue S, Becker AE, Riccardi R, Gaita F. Interruption of the inferior extension of the compact atrioventricular node underlies successful radio frequency ablation of atrioventricular nodal reentrant tachycardia. J Interv Card Electrophysiol. 1999 Oct;3(3):273-7.
13. Inoue S, Becker A. Posterior extensions of the human compact atrioventricular node. A neglected anatomic feature of potential clinical significance. Circulation. 1998;97:188-193.
14. Katritsis DG, Becker A. The atrioventricular nodal reentrant tachycardia circuit: a proposal. Heart Rhythm. 2007 Oct;4(10):1354-60.
15. Chugh A, Oral H, Good E, Han J, Tamirisa K, Lemola K, Elmouchi D, Tschopp D, Reich S, Igic P, Bogun F, Pelosi F Jr, Morady F. Catheter ablation of atypical atrial flutter and atrial tachycardia within the coronary sinus after left atrial ablation for atrial fibrillation. J Am Coll Cardiol. 2005 Jul 5;46(1):83-91.
16. Olgin JE, Jayachandran JV, Engesstein E, Groh W, Zipes DP. Atrial macroreentry involving the myocardium of the coronary sinus: a unique mechanism for atypical flutter. J Cardiovasc Electrophysiol. 1998 Oct;9(10):1094-9.
17. Asirvatham SJ. Correlative Anatomy and Electrophysiology for the Interventional Electrophysiologist: Right Atrial Flutter. J Cardiovasc Electrophysiol. 2009 Jan;20(1):113-22.
18. Haïssaguerre M, Jaïs P, Shah DC, Takahashi A, Hocini M, Quiniou G, Garrigue S, Le Mouroux A, Le Métayer P, Clémenty J. Spontaneous initiation of atrial fibrillation by ectopic beats originating in the pulmonary veins. N Engl J Med. 1998 Sep 3;339(10):659-66.
19. Saad EB, Marrouche NF, Saad CP, Ha E, Bash D, White RD, Rhodes J, Prieto L, Martin DO, Saliba WI, Schweikert RA, Natale A.Pulmonary vein stenosis after catheter ablation of atrial fibrillation: emergence of a new clinical syndrome.Ann Intern Med. 2003 Apr 15;138(8):634-8.
20. Tse HF, Reek S, Timmermans C, Lee KL, Geller JC, Rodriguez LM, Ghaye B, Ayers GM, Crijns HJ, Klein HU, Lau CP. Pulmonary vein isolation using transvenous

catheter cryoablation for treatment of atrial fibrillation without risk of pulmonary vein stenosis. J Am Coll Cardiol. 2003 Aug 20;42(4):752-8.

21. Hirao K, Otomo K, Wang X, Beckman KJ, McClelland JH, Widman L, Gonzalez MD, Arruda M, Nakagawa H, Lazzara R, Jackman WM. Para-Hisian pacing. A new method for differentiating retrograde conduction over an accessory AV pathway from conduction over the AV node. Circulation. 1996 Sep 1;94(5):1027-35.
22. Sadler TW. Development of the sinus venosus. In: Langman's Medical Embryology. 7th ed. Balimore, Md: Williams & Wilkins; 1995:188-191.
23. Wen MS, Yeh SJ, Wang CC, King A, Lin FC, Wu D. Radiofrequency ablation therapy of the posteroseptal accessory pathway. Am Heart J. 1996 Sep;132(3):612-20.
24. Akiyama M, Kaneko Y, Taniguchi Y, Nakajima T, Manita M, Ito T, Saito A, Kurabayashi M. Coronary sinus recordings of double potentials associated with retrograde conduction through left atrioventricular accessory pathways. J Cardiovasc Electrophysiol. 2004 Dec;15(12):1371-6.
25. Uchida F, Fujii E, Matsuoka K, Okubo S, Kasai A, Omichi C, Nakano T. Effect of left atrial-coronary sinus musculature connections on the coronary sinus activation pattern via retrograde conduction in patients with WPW syndrome. J Interv Card Electrophysiol. 2004 Feb;10(1):59-64.
26. Reddy GV, Schamroth L. The localization of bypass tracts in the Wolff-Parkinson-White syndrome from the surface electrocardiogram. Am Heart J. 1987 Apr;113(4):984-93.
27. Fitzpatrick AP, Gonzales RP, Lesh MD, Modin GW, Lee RJ, Scheinman MM. New algorithm for the localization of accessory atrioventricular connections using a baseline electrocardiogram. J Am Coll Cardiol. 1994 Jan;23(1):107-16.
28. Dhala AA, Deshpande SS, Bremner S, Hempe S, Sra JS, Blanck Z, Akhtar M, Jazayeri MR. Transcatheter ablation of posteroseptal accessory pathways using a venous approach and radiofrequency energy. Circulation. 1994 Oct;90(4):1799-810.
29. Arruda MS, McClelland JH, Wang X, Beckman KJ, Widman LE, Gonzalez MD, Nakagawa H, Lazzara R, Jackman WM. Development and validation of an ECG algorithm for identifying accessory pathway ablation site in Wolff-Parkinson-White syndrome. J Cardiovasc Electrophysiol. 1998 Jan;9(1):2-12.

30. Takahashi A, Shah DC, Jaïs P, Hocini M, Clementy J, Haïssaguerre M. Specific electrocardiographic features of manifest coronary vein posteroseptal accessory pathways. J Cardiovasc Electrophysiol. 1998 Oct;9(10):1015-25.
31. Kobza R, Hindricks G, Tanner H, Piorkowski C, Wetzel U, Schirdewahn P, Dorszewski A, Gerds-Li JH, Kottkamp H. Paraseptal accessory pathway in Wolff-Parkinson- White-Syndrom: ablation from the right, from the left or within the coronary sinus/middle cardiac vein? J Interv Card Electrophysiol. 2005 Jan;12(1):55-
32. Extramiana F, Takatsuki S, Hayashi M, Leenhardt A. Functional bundle branch block and orthodromic reciprocating tachycardia cycle length: do not bet on accessory pathway location. Europace. 2007 Oct;9(10):920-2.
33. Chiang CE, Chen SA, Tai CT, Wu TJ, Lee SH, Cheng CC, Chiou CW, Ueng KC, Wen ZC, Chang MS. Prediction of successful ablation site of concealed posteroseptal accessory pathways by a novel algorithm using baseline electrophysiological parameters: implication for an abbreviated ablation procedure. Circulation. 1996 Mar 1;93(5):982-91.
34. Hussin A, Sanders P, Kistler PM, Sparks PB, Kalman JM. Accessory pathway in left inferoposterior diverticulum masquerading as left posterior pathway due to conduction over coronary sinus to left atrium connection. J Cardiovasc Electrophysiol. 2003 Apr;14(4):403-6.
35. Gatzoulis KA, Apostolopoulos T, Costeas X, Zervopoulos G, Papafanis F, Sotiropoulos H, Gialafos J, Toutouzas P. Radiofrequency catheter ablation of posteroseptal accessory pathways--results of a step-by-step ablation approach. J Interv Card Electrophysiol. 2001 Jun;5(2):193-201.
36. Ticho BS, Saul JP, Hulse JE, De W, Lulu J, Walsh EP. Variable location of accessory pathways associated with the permanent form of junctional reciprocating tachycardia and confirmation with radiofrequency ablation. Am J Cardiol. 1992 Dec 15;70(20):1559-64.
37. Gaita F, Haissaguerre M, Giustetto C, Fischer B, Riccardi R, Richiardi E, Scaglione M, Lamberti F, Warin JF. Catheter ablation of permanent junctional reciprocating tachycardia with radiofrequency current. J Am Coll Cardiol. 1995 Mar 1;25(3):648-54.

38. Meiltz A, Weber R, Halimi F, Defaye P, Boveda S, Tavernier R, Kalusche D, Zimmermann M; Reseau Europeen pour le Traitement des Arythmies Cardiaques. Permanent form of junctional reciprocating tachycardia in adults: peculiar features and results of radiofrequency catheter ablation. Europace. 2006 Jan;8(1):21-8.
39. McGuire MA. A Simple, Clinically Useful Technique to Predict Successful Ablation Site of Accessory Pathways Located Near the Cardiac Septum? J Cardiovasc Electrophysiol. 2008 Jul;19(7):659-660.
40. Morady F. Treatment of paroxysmal atrial fibrillation by pulmonary vein isolation. Circ J. 2003 Jul;67(7):567-71.
41. Cappato R, Negroni S, Pecora D, Bentivegna S, Lupo PP, Carolei A, Esposito C, Furlanello F, De Ambroggi L. Prospective assessment of late conduction recurrence across radiofrequency lesions producing electrical disconnection at the pulmonary vein ostium in patients with atrial fibrillation. Circulation. 2003 Sep 30;108(13):1599-604.
42. Pappone C, Oral H, Santinelli V, Vicedomini G, Lang CC, Manguso F, Torracca L, Benussi S, Alfieri O, Hong R, Lau W, Hirata K, Shikuma N, Hall B, Morady F: Atrio-esophageal fistula as a complication of percutaneous transcatheter ablation of atrial fibrillation. Circulation 2004;109: 2724-2726.
43. Friedman PL. Catheter cryoablation of cardiac arrhythmias. Curr Opin Cardiol. 2005 Jan;20(1):48-54.
44. Doll N, Borger MA, Fabricius A, Stephan S, Gummert J, Mohr FW, Hauss JJ, Kottkamp H, Hindricks G: Esophageal perforation during left atrial radio frequency ablation: Is the risk too high?J Thorac Cardiovasc Surg 2003;125: 836-842.
45. Cappato R, Calkins H, Chen SA, Davies W, Iesaka Y, Kalman J, Kim YH, Klein G, Packer D, Skanes A: Worldwide survey on the methods, efficacy, and safety of catheter ablation for human atrial fibrillation. Circulation 2005;111: 1100-1105.
46. Ouyang F, Antz M, Ernst S, Hachiya H, Mavrakis H, Deger FT, Schaumann A, Chun J, Falk P, Hennig D, Liu X, Bansch D, Kuck KH: Recovered pulmonary vein conduction as a dominant factor for recurrent atrial tachyarrhythmias after complete circular isolation of the pulmonary veins. Lessons from double Lasso technique. Circulation 2005;111: 127-135.

47. Siklódy CH, Minners J, Allgeier M, Allgeier HJ, Jander N, Weber R, Schiebeling-Römer J, Neumann FJ, Kalusche D, Arentz T. Cryoballoon Pulmonary Vein Isolation Guided by Transesophageal Echocardiography: Novel Aspects on an Emerging Ablation Technique. J Cardiovasc Electrophysiol. 2009 Jun 26. [Epub ahead of print]
48. Linhart M, Bellmann B, Mittmann-Braun E, Schrickel JW, Bitzen A, Andrié R, Yang A, Nickenig G, Lickfett L, Lewalter T. Comparison of Cryoballoon and Radiofrequency Ablation of Pulmonary Veins in 40 Patients with Paroxysmal Atrial Fibrillation: A Case-Control Study. J Cardiovasc Electrophysiol. 2009 Jul 28. [Epub ahead of print]

Acknowledgements

I would like to thank my tutor and supervisor Professor Tamás Forster for directing my scientific work. I am grateful to Dr. László Sághy, director of the Szeged EP lab, for his efforts and support with the studies and all the staff of the EP lab, for their continuous help. I would also like to express my gratitude to Dr. Zoltán Csanádi and towards the Arrhythmia Service at the University of Western Ontario, especially doctors Allan Skanes and George Klein. Last, but not least I thank my wife and kids for their support.